AIMS Mathematics, 10(7): 17117–17178.
DOI: 10.3934/math.2025768
Received: 14 June 2025
Revised: 22 July 2025
Accepted: 24 July 2025
Published: 31 July 2025

http://www.aimspress.com/journal/Math

Research article

The discrete Gompertz–Makeham distribution for multidisciplinary data analysis

Ahmed Elshahhat[1,*], **Hoda Rezk**[2] **and Refah Alotaibi**[3]

[1] Faculty of Technology and Development, Zagazig University, Zagazig 44519, Egypt
[2] Department of Statistics, Al-Azhar University, Cairo, Egypt
[3] Department of Mathematical Sciences, College of Science, Princess Nourah bint Abdulrahman University, P.O. Box 84428, Riyadh 11671, Saudi Arabia

* **Correspondence:** Email: aelshahhat@ftd.zu.edu.eg; Tel: +201225939600.

Abstract: The Gompertz–Makeham (GM) distribution has the flexibility to model real-world lifetime data with increasing, decreasing, or constant hazard rates, making it exceptionally valuable for applications in survival analysis, actuarial science, demography, and reliability engineering. This study proposes and rigorously analyzes a novel discrete formulation of the classical GM distribution, tailored to address real-world applications where event times are inherently discrete. Utilizing the survival function discretization technique, the authors derive the discrete GM (DGM) model and establish its foundational probability mass function, hazard rate function, and cumulative distribution function. A comprehensive suite of statistical properties—including quantiles, moments, skewness, kurtosis, and order statistics—is developed and examined numerically. Recognizing the challenges of parameter estimation under Type–II data censoring, the paper implements both maximum likelihood estimation and Bayesian inference, with the latter incorporating gamma priors and executed via a Metropolis–Hastings Markov chain Monte Carlo algorithm. The paper further evaluates the estimator's performance through extensive simulations. The findings consistently demonstrate the superiority of Bayesian methods, particularly with high posterior density intervals. From three life sciences, several empirical case studies underscore the practical utility of the DGM model, showcasing improved goodness-of-fit relative to existing discrete models, for example, the discrete Nadarajah–Haghighi, discrete modified Weibull, discrete Weibull, and discrete gamma models, among others. Finally, this work fills a notable gap in the literature by extending the GM framework to discrete domains with full inferential machinery.

Keywords: discrete Gompertz–Makeham; likelihood; Bayesian; Markovian chains; censoring; failure rate; order statistics; real-world data modelling
Mathematics Subject Classification: 60E05, 62E10, 62N01, 62N05, 62P10

1. Introduction

The Gompertz–Makeham (GM) distribution stands as one of the foundational models in survival analysis, demography, and reliability theory, with origins tracing back to Benjamin Gompertz's seminal work in 1825 (see Gompertz [1]) and William Makeham's additive refinement in 1860 (see Makeham [2]). Originally designed to describe the rapid increase in human mortality with age, the GM model combines a constant hazard with an age-related component and accounts for both random shocks and systematic aging, making it a flexible and understandable framework for modeling time-to-event data. Over the decades, its adaptability has extended beyond human lifespans to encompass failure times in biological systems, industrial components, and financial risk processes. Mathematically, the GM hazard function, say $h(\cdot)$, is defined as $h(t) = A + BC^t$, where $A = \alpha > 0$ captures age-independent mortality (Makeham term), $B = \theta > 0$, and $C = e^{\mu}$, $\mu > 0$, while the exponential term BC^t models age-dependent risk escalation (Gompertz term). Over the decades, the adaptability of the GM distribution has extended beyond modeling human lifespans to encompass failure times in biological systems, industrial components, and financial risk processes; for more details, see Marshall and Olkin [3]. Its applications span various fields, for example:

- Actuarial science – modeling mortality rates, estimating life expectancy, and pricing insurance products (see Shilovsky [4]);
- Biology – examining mortality patterns in various human populations (see Castellares et al. [5]);
- Demography – analyzing population aging, predicting population trends, and studying mortality patterns across different populations (see Souza [6]);
- Gerontology – exploring the aging process and age-related diseases (see Missov and Lenart [7]);
- Computer science – modeling the failure rates of computer systems and software to improve predictions of systems'behavior and reliability (see Bajjouk et al. [8]);
- Marketing science – simulating individual customers' behavior, particularly in the context of customer lifetime value (see Huang et al. [9]), among others.

Discretizing continuous distributions serves both theoretical and practical purposes, especially in modern applications where data are naturally recorded in integer-valued or interval-based formats. Many classical models in survival analysis and reliability theory, such as the GM distribution, are inherently continuous in nature and thus are not directly compatible with discrete data arising from digital sensors, count processes, or grouped observations. By constructing discrete analogues, we preserve the essential structural properties (e.g., monotonic hazard behavior, tail flexibility) of the continuous models while adapting them to suit the data constraints. This not only facilitates proper likelihood-based inference but also avoids the pitfalls of discretization by rounding or binning, which can introduce bias or inefficiency. Furthermore, discrete distributions often offer computational advantages, closed-form expressions for probabilities, and improved model interpretability in domains such as reliability engineering, queueing systems, epidemiology, and actuarial science. Thus, the development of discrete counterparts to well-established continuous models plays a vital role in expanding the scope of probabilistic modeling under realistic data conditions; see Keefer and Bodily [10] for additional details. Several continuous lifespan distributions have recently been discretized in literature due to the need for more dependable discrete distributions that can replicate discrete data in a variety of real-world situations; for further details, see Lai [11] and Chakraborty [12].

Recently, several works have made significant contributions to the development of discrete reliability theory by introducing new perspectives and methods. Several partitioning techniques are used to transform continuous models into their discrete equivalents, and these techniques are widely studied and documented in the scientific literature. The goal of these techniques is to produce discrete distributions that closely resemble their continuous sources. A variety of discretization techniques have been examined in the literature; in this context, Hammond and Bickel [13] offer a brief review.

A prominent method in the creation of discrete distributions is the use of the survival function as a discretization technique. Notable contributions in this field include the derivation of discrete analogs for the normal and Rayleigh distributions, which were presented by Roy [14, 15], both of which used the survival function methodology. Building on this framework, Bebbington et al. [16] conducted a thorough investigation of the discrete additive counterpart of the Weibull distribution.

Despite the GM distribution's great adaptability in various sciences in a continuous framework, real-world applications frequently use data that have been censored or recorded at discrete intervals. For example, in cases of patient deaths, medical follow-up periods, or the number of failures in industrial tests, data are collected in discrete time units, e.g., when modeling the number of periods until death or disability, the number of use cycles until a system fails, the number of accidents, or student grades, among others. Nevertheless, the corresponding discrete version of the continuous GM distribution has not yet been proposed in the literature. Given the increasing prevalence of discrete-time data in modern applications, the goal of this research is to close this distribution theory gap. In the next section, we discretize the GM distribution to facilitate the analysis of discrete event data subject to complete and/or incomplete sampling, such as Type II censoring. The limitation of the study is discretizing the GM model using the survival function approach, along with the derivation of several theoretical constraints, comparisons of data fit, and computational aspects related to estimation and inference. We now list the five main contributions of the study as follows:

- The proposed discrete GM (DGM) distribution maintains the key features of the continuous GM model, such as its additive exponential hazard form.
- Several important mathematical characteristics of the DGM distribution, including probability mass, cumulative distribution, survival, hazard rate, and quantile functions, along with moments and order statistics, support its theoretical validity and interpretability.
- The Bayesian framework and maximum likelihood estimation technique are applied under both complete and incomplete (Type–II censoring) sampling schemes, demonstrating the model's flexibility in realistic reliability testing scenarios.
- Monte Carlo simulations are performed to evaluate the behavior of the estimators under different censoring conditions, emphasizing the model's practical utility and inferential stability.
- To verify the flexibility and superior fit of the DGM distribution and to confirm its effectiveness in modeling discrete-time failure data across clinical, engineering, and physical sectors, the results indicate that the DGM outperforms other recently proposed discrete versions of common continuous distributions, including the modified Weibull, Nadarajah–Haghighi, Burr Type XII, Weibull, and gamma models, and others.

The remainder of the paper is structured as follows: Section 2 introduces the proposed DGM distribution, while Section 3 presents its key properties and features. Parameter estimation is addressed in Sections 4 and 5. Section 6 reports the simulation results. In Section 7, three real-world datasets are analyzed. Finally, Section 8 ends the paper with a summary of the findings and future research.

2. The DGM Distribution

Recall that the GM lifespan model is widely used in fields such as reliability engineering, actuarial science, and demography. It combines two components to model time to failure (or death): (i) Gompertz's law of mortality, which represents a hazard that increases exponentially with age, and (ii) Makeham's constant risk, which accounts for age-independent hazards. The GM distribution is particularly useful in life insurance modeling, human longevity studies, and the analysis of aging mechanical systems; see Cohen [17]. As such, it remains a fundamental tool for modeling survival data with increasing hazard rates across a wide range of scientific domains. We are excited to use the GM model because of its flexibility in detecting random failures early in life, as well as the rapidly increasing risk of death or failure later in life. Other reasons we rely on to consider this lifespan model are that its density function is tractable and allows for smooth and realistic modeling of lifetimes, while its failure rate function (HRF) makes it simpler to capture the constant tail risk and control for the age-dependent component. The probability density function (say, $f(\cdot)$) and the survival function (say, $S(\cdot)$) of a random variable X that follows the three-parameter GM model are defined as follows:

$$f(x;\boldsymbol{\zeta}) = (\alpha + \theta e^{\mu x}) \exp\left(-\alpha x - \frac{\theta}{\mu}(e^{\mu x} - 1)\right),\ x > 0, \tag{2.1}$$

and

$$S(x;\boldsymbol{\zeta}) = \exp\left(-\alpha x - \frac{\theta}{\mu}(e^{\mu x} - 1)\right), \tag{2.2}$$

respectively, where $\boldsymbol{\zeta} = (\alpha, \theta, \mu)^\top$. Several discretization techniques exist for deriving discrete analogues of continuous distributions, with survival function-based discretization being one of the most prominent. Next, we adopt the survival-based estimation approach to construct the probability mass function (PMF), cumulative distribution function (CDF), and related properties of the DGM model.

2.1. The PMF and its log-concavity

Following Roy [14, 15], the DGM's PMF using survival discretization is defined as:

$$\begin{aligned} P(Z = z) &= S(z) - S(z+1), \\ &= \Delta(\alpha, \theta, \mu; (z)) - \Delta(\alpha, \theta, \mu; (z+1)),\ z = 0, 1, 2, ... \end{aligned} \tag{2.3}$$

where $\Delta(\alpha, \theta, \mu; (z)) = e^{-\alpha(z) - \frac{\theta}{\mu}(e^{\mu z} - 1)}$ and $\Delta(\alpha, \theta, \mu; (z+1)) = e^{-\alpha(z+1) - \frac{\theta}{\mu}(e^{\mu(z+1)} - 1)}$.

The DGM distribution possesses a log-concave PMF, implying it is unimodal and structurally stable under convolution; see Theorem 1. This property enhances its applicability in modeling real-world lifetime data with consistent probabilistic behavior.

Theorem 1. *Let Z be a discrete random variable following the DGM distribution with the survival discretization function $\Delta(z) = \exp\left(-\alpha z - \frac{\theta}{\mu}(e^{\mu z} - 1)\right)$, $z \in \mathbb{N}_0$, and $\alpha, \theta, \mu > 0$. Then, the corresponding PMF $P(z) = \Delta(z) - \Delta(z+1)$ is log-concave. That is, $P(z)^2 \geq P(z-1) \cdot P(z+1)$ for all $z \geq 1$. Specifically, the second-order difference of $\log \Delta(z)$ is given by:*

$$\mathrm{d}^2 \log \Delta(z) = \frac{\theta}{\mu} e^{\mu z} \left(-e^{\mu} + 2 - e^{-\mu}\right),$$

in a way that $\log \Delta(z)$ is concave; hence $\Delta(z)$ is log-concave, and so is $P(z)$.

Proof. See Appendix A.

2.2. The CDF and HRF

From (2.3), the respective CDF and HRF of the newly DGM model are:

$$\begin{aligned} F(z) &= P(Z \leqslant z) \\ &= 1 - S(z) + P(Z = z) \\ &= 1 - \Delta(\alpha, \theta, \mu; (z+1)), \quad \alpha, \theta, \mu > 0,\ z = 0, 1, 2, \ldots \end{aligned} \tag{2.4}$$

and

$$\begin{aligned} h(z) &= \frac{P(z)}{S(z)} \\ &= 1 - \frac{\Delta(\alpha, \theta, \mu; (z+1))}{\Delta(\alpha, \theta, \mu; (z))}, \\ &= 1 - \exp\left(-\alpha - \frac{\theta}{\mu}\left(e^{\mu(z+1)} - e^{\mu z}\right)\right), \quad \alpha, \theta, \mu > 0,\ z = 0, 1, 2, \ldots, \end{aligned} \tag{2.5}$$

where α, θ, and μ denote the DGM's parameters.

Figure 1 illustrates various shapes of the PMF and HRF for the DGM distribution, generated using different parameter selections. The subplots in Figure 1(a) illustrate the flexibility of the new DGM distribution in capturing various PMF shapes, including increasing (right-skewed), decreasing (left-skewed), and unimodal forms. The subplots in Figure 1(b), by fixing $\alpha = 1$ and $\theta = 0.1$, illustrate that all HRF shapes of the DGM are monotonically increasing.

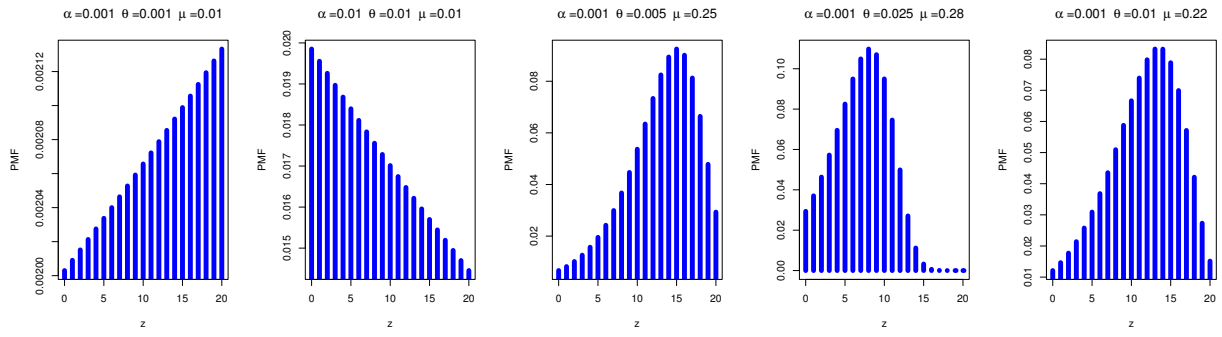

(a) PMF

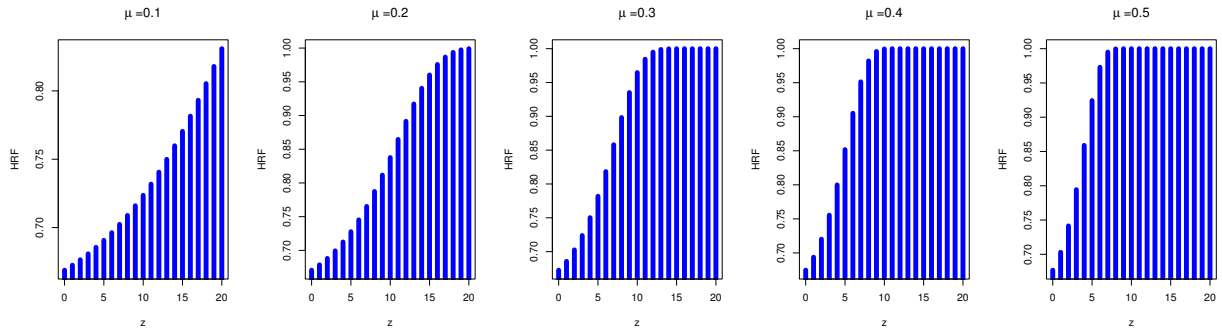

(b) HRF

Figure 1. The PMF and HRF shapes of the DGM distribution.

It should be noted here that although α is included in the HRF expression (2.5), it does not influence the shape (monotonicity) of the hazard function. Instead, it acts as a constant additive term in the exponent, shifting the hazard rate up or down uniformly across all time points. The increasing behavior of $h(z)$ is governed entirely by the exponential term $e^{\mu z}$, which increases with z due to $\mu > 0$ and $\theta > 0$. Thus, the monotonicity and shape of the hazard function are controlled by θ and μ, while α only affects its level. As detailed in Theorem 2, the DGM distribution is shown to provide an increasing failure rate (IFR).

Theorem 2. *The HRF $h(z)$ is monotonically increasing, and the DGM distribution exhibits the IFR property for all $\alpha, \theta, \mu > 0$. Let Z be a discrete random variable following the DGM distribution with the parameters $\alpha, \theta, \mu > 0$. Then, the HRF given by*

$$h(z) = 1 - \exp\left(-\alpha - \frac{\theta}{\mu} e^{\mu z}(e^{\mu} - 1)\right), \quad z \in \mathbb{N}_0,$$

is strictly increasing in z. That is,

$$h(z+1) > h(z), \quad \textit{for all } z \geq 0.$$

Proof. We first re-express HRF (2.5) as follows:

$$h(z) = 1 - \exp(-\varphi(z)),$$

where $\varphi(z) := \alpha + \frac{\theta}{\mu} e^{\mu z}(e^{\mu} - 1)$.

We now consider the first-order forward difference of $\varphi(z)$, say $\varphi^{\star}(z)$, as follows:

$$\begin{aligned} \varphi^{\star}(z) &= \varphi(z+1) - \varphi(z) \\ &= \frac{\theta}{\mu}\left(e^{\mu(z+1)} - e^{\mu z}\right)(e^{\mu} - 1), \end{aligned}$$

hence,

$$\varphi^{\star}(z) = \frac{\theta}{\mu} e^{\mu z}(e^{\mu} - 1)^2 > 0 \quad \text{for all } z \geq 0,$$

since $\theta > 0$, $\mu > 0$, and $e^{\mu} > 1$.

Therefore, $\varphi(z)$ is strictly increasing in z. Since $h(z) = 1 - \exp(-\varphi(z))$ is a strictly increasing transformation of $\varphi(z)$, it follows that $h(z)$ is strictly increasing in z as well. □

Remark 1: The DGM distribution exhibits an IFR, making it well-suited for modeling lifetime data with aging effects. Its hazard function closely resembles that of the continuous GM distribution, with both showing time-dependent growth consistent with reliability and survival contexts. In the next section, several additional statistical properties and characteristics of the DGM model, such as its quantiles, moments, and ordered statistics, are derived.

3. Statistical functions

The quantile function, moments, skewness, kurtosis, and order statistics are among the statistical functions of the DGM distribution that are covered in this section.

3.1. Quantiles and moments

The quantile function (say, $Q(u)$) for a discrete distribution is the inverse of its CDF. It is used basically to generate random samples for simulation purposes. To determine the quantile function, we solve for z in terms of u as follows:

$$u = 1 - \Delta(\alpha, \theta, \mu; (z + 1)). \tag{3.1}$$

Equation (3.1) can be rearranged to obtain

$$\Delta(\alpha, \theta, \mu; (z + 1)) = 1 - u. \tag{3.2}$$

When $\Delta(\alpha, \theta, \mu; (z + 1))$ is substituted into Eq (3.2), we obtain

$$\left(-\alpha(z + 1) - \frac{\theta}{\mu}(e^{\mu(z+1)} - 1)\right) = 1 - u, \tag{3.3}$$

and the natural logarithm of (3.3) becomes

$$-\alpha(z + 1) - \frac{\theta}{\mu}\left(e^{\mu(z+1)} - 1\right) = \log(1 - u). \tag{3.4}$$

This problem needs to be solved numerically, since the combination of logarithmic and exponential terms usually makes an analytical closed-form statement impractical. Due to the complexity of the DGM distribution's cumulative distribution, deriving the quantile function in explicit form is infeasible, particularly when both exponential and power components are involved. The process of extracting z from the expression for $\Delta(z, \zeta)$ presents significant analytical challenges and is unlikely to provide a precise answer due to the complex structure and exponential decay term. Approximations or numerical techniques can be used for practical applications as an alternative to the traditional analytical form. Moments are essential statistical tools that provides in-depth information on the characteristics and form of a probability distribution.

To calculate the DGM model's moments, consider the non-negative random variable $w \sim DGM(\zeta)$. The following s-th is an expression for the moment, say μ'_s:

$$\mu'_s = \sum_{w=0}^{\infty} w^s \left\{\Delta(\alpha, \theta, \mu; (w)) - \Delta(\alpha, \theta, \mu; (w + 1))\right\}. \tag{3.5}$$

Since there is no precise expression for the moment, numerical approaches must be used to assess it. To examine the probabilistic characteristics of the DGM distribution, we explored a range of parameter configurations, specifically selecting the values $\alpha \in \{0.25, 0.75, 1.5\}$ and varying θ and μ accordingly. Table 1 presents the resulting summary measures, including the mean (M), variance (V), index of dispersion (ID), coefficient of variation (CV), skewness (S), and kurtosis (K). It exhibits that as α grows (for fixed θ and μ), the estimated values of M, V, and ID tend to decrease, while those of CV, S, and K tend to increase. Similar behavior can also be observed when θ (or μ) grows while keeping the other parameters constant.

Table 1. Vital metrics of the DGM using several values of its parameters.

α	θ	μ	M	V	ID	CV	S	K
0.25	0.5	0.1	0.7907	1.2285	1.5537	1.3690	1.1090	2.6162
		0.5	0.5310	0.5285	0.9952	1.4018	1.2242	3.1794
		1.0	0.3547	0.2788	0.7858	1.4883	1.2393	3.9668
		1.5	0.2451	0.1871	0.7635	1.7651	1.7655	6.7860
		2.5	0.0832	0.0763	0.9168	3.3195	3.0183	10.110
	1.5	0.1	0.1854	0.2063	1.1126	2.4495	2.6656	11.018
		0.5	0.1147	0.1086	0.9991	2.8725	2.7116	9.4325
		1.0	0.0592	0.0558	0.9760	3.9892	3.7449	15.077
		1.5	0.0240	0.0234	0.9468	6.3835	6.2269	39.774
		2.5	0.0009	0.0009	0.9422	32.436	32.405	1051.1
0.75	0.5	0.1	0.3767	0.4908	1.3030	1.8599	1.7737	5.0527
		0.5	0.2903	0.2995	1.0319	1.8855	1.8697	5.1093
		1.0	0.2092	0.1838	0.9495	2.0490	2.0037	6.2235
		1.5	0.1484	0.1271	0.8784	2.4030	2.2424	9.2619
		2.5	0.0505	0.0479	0.8568	4.3378	4.1072	17.869
	1.5	0.1	0.1062	0.1134	1.0684	3.1721	3.3603	15.298
		0.5	0.0688	0.0666	0.9994	3.7539	3.6334	15.395
		1.0	0.0359	0.0346	0.9855	5.1844	4.9963	26.014
		1.5	0.0145	0.0143	0.9689	8.2361	8.1147	66.848
		2.5	0.0006	0.0006	0.9650	41.657	41.633	1734.3
1.50	0.5	0.1	0.1505	0.1700	1.1293	2.7392	2.9023	10.617
		0.5	0.1259	0.1293	1.0270	2.8560	2.9524	11.543
		1.0	0.0965	0.0913	0.9458	3.1299	3.0399	12.547
		1.5	0.0700	0.0653	0.9325	3.6499	3.3862	13.816
		2.5	0.0238	0.0233	0.9762	6.3993	6.2430	39.975
	1.5	0.1	0.0479	0.0495	1.0322	4.6406	4.7806	27.110
		0.5	0.0322	0.0317	0.9997	5.5368	5.4568	31.890
		1.0	0.0170	0.0167	0.9931	7.6161	7.4880	57.119
		1.5	0.0069	0.0068	0.9858	12.030	11.947	143.73
		2.5	0.0003	0.0003	0.9834	60.619	60.603	3673.7

Remark 2: The consistently positive skewness of the DGM distribution indicates its suitability for modeling right-skewed data, while high kurtosis reflects the model's ability to detect heavy tails and peaks, which are important features in reliability contexts. Moreover, the variance-to-mean ratio confirms that the DGM distribution accommodates both over- and under-dispersion, enhancing its adaptability compared with classical models like the Poisson model.

3.2. Order statistics

Let $(Z_1, Z_2, \ldots, Z_n)$ be a random sample from the DGM model, and let $(Y_{1:m}, Y_{2:m}, \ldots, Y_{n:m})$ be the associated order statistics. As a result, the i-order statistics have a CDF at y and can be represented as

$$F_{i:n}(y;\zeta) = \sum_{i=1}^{n} \binom{n}{m} [F_i(y;\zeta)]^m [1 - F_i(y;\zeta)]^{n-m}. \tag{3.6}$$

The negative binomial theorem can be used as a series representation of (3.6) as follows:

$$F_{i:n}(y;\zeta) = \sum_{i=1}^{n} \sum_{j=1}^{n-m} \binom{n}{m} \binom{n-m}{j} (-1)^j [F_i(y;\zeta)]^{m+j}. \tag{3.7}$$

Consequently, where $\Delta(y;\boldsymbol{\zeta}) = \exp\left(-\alpha(y+1) - \frac{\theta}{\mu}(e^{\mu(y)} - 1)\right)$, we get

$$F_{i:n}(y;\zeta) = \sum_{i=1}^{n} \sum_{j=1}^{n-m} \binom{n}{m} \binom{n-m}{j} (-1)^j \left[1 - \Delta(y;\boldsymbol{\zeta})\right]^{m+j}. \tag{3.8}$$

The PMF for the i-th order statistic in the DGM model can be expressed as follows:

$$f_{i:n}(y;\zeta) = \sum_{i=1}^{n}\sum_{j=1}^{n-m}\binom{n}{m}\binom{n-m}{j}(-1)^j\left[\Delta(y;\boldsymbol{\zeta}) - \Delta(y+1;\boldsymbol{\zeta})\right]^{m+j}. \tag{3.9}$$

Thus, the following is a possible way to write the r-th moment of $Y_{i:n}$:

$$\mathbb{E}(Y_{i:n}^r) = \sum_{y=0}^{\infty}\sum_{i=1}^{n}\sum_{j=1}^{n-m}\binom{n}{m}\binom{n-m}{j}(-1)^j y^r\left[\Delta(y;\boldsymbol{\zeta}) - \Delta(y+1;\boldsymbol{\zeta})\right]^{m+j}. \tag{3.10}$$

Order statistics are particularly important for evaluating the behavior of a distribution under extreme values. To examine the tails of the distribution, we focus on the minimum and maximum order statistics. These correspond to $i \to 1$ and n in Eq (3.9), and their distributions provide insight into early failures and long-lived components, respectively. These expressions are particularly useful for studying early failure behavior in reliability applications. However, from (3.9), we obtain simplified expressions for the two extreme order statistics, namely the minimum and maximum order statistics (at $i = 1$ and $i = n$), respectively, as follows:

- The PMF of minimum order statistic ($Z_{(1)}$)

$$\begin{aligned} f_{1:n}(y;\boldsymbol{\zeta}) &= [\Delta(y;\boldsymbol{\zeta})]^n - [\Delta(y+1;\boldsymbol{\zeta})]^n \\ &= [1 - F(y;\boldsymbol{\zeta})]^n - [1 - F(y+1;\boldsymbol{\zeta})]^n. \end{aligned}$$

- The PMF of maximum order statistic ($Z_{(n)}$)

$$f_{n:n}(y;\boldsymbol{\zeta}) = [F(y;\boldsymbol{\zeta})]^n - [F(y-1;\boldsymbol{\zeta})]^n.$$

Using varying configurations of the sample sizes (n) and parameter settings ($\boldsymbol{\zeta}$), the numerical evaluations of $\mathbb{E}[Z_{(1)}]$ and $\mathbb{E}[Z_{(n)}]$ (reported in Table 2), where 7.99E-03 implies $0.00799 \simeq 7.99 \times 10^{-3}$ (for example), illustrate the tail behavior of the DGM distribution through the expected minimum and maximum order statistics. This property is vital for modeling various reliability scenarios.

Table 2. The results of $\mathbb{E}[Z_{(1)}]$ (1^{st} Col.) and $\mathbb{E}[Z_{(n)}]$ (2^{nd} Col.) from DGM($\boldsymbol{\zeta}$) model.

$n \downarrow (\alpha,\theta,\mu) \rightarrow$	(0.1,0.1,0.1)		(0.2,0.5,0.8)		(1,0.1,0.1)		(0.1,1,0.1)		(0.1,0.1,1)	
5	5.35E-01	5.13E+00	7.99E-03	2.17E+00	4.00E-03	2.55E+00	3.16E-03	2.36E+00	2.72E-01	3.40E+00
10	1.45E-01	4.21E+00	6.38E-05	2.44E+00	1.59E-05	3.12E+00	9.96E-06	2.85E+00	6.62E-02	3.72E+00
20	1.67E-02	2.33E+00	4.07E-09	2.71E+00	2.52E-10	3.71E+00	9.92E-11	3.33E+00	4.35E-03	3.96E+00
50	3.51E-05	3.21E-01	1.06E-21	3.00E+00	1.00E-24	4.49E+00	9.79E-26	3.94E+00	1.25E-06	4.14E+00
80	7.44E-08	4.21E-02	2.75E-34	3.07E+00	4.00E-39	4.90E+00	9.67E-41	4.25E+00	3.60E-10	4.22E+00
100	1.23E-09	1.08E-02	1.12E-42	3.10E+00	1.01E-48	5.09E+00	9.59E-51	4.39E+00	1.57E-12	4.27E+00
150	4.31E-14	3.57E-04	1.18E-63	3.14E+00	1.01E-72	5.43E+00	9.39E-76	4.64E+00	1.96E-18	4.38E+00
200	1.51E-18	1.18E-05	1.25E-84	3.19E+00	1.01E-96	5.67E+00	9.20E-101	4.82E+00	2.45E-24	4.47E+00
250	5.29E-23	3.87E-07	1.32E-105	3.23E+00	1.02E-120	5.86E+00	9.01E-126	4.95E+00	3.07E-30	4.55E+00
300	1.86E-27	1.28E-08	1.40E-126	3.27E+00	1.02E-144	6.01E+00	8.83E-151	5.06E+00	3.84E-36	4.61E+00

Remark 3: As n grows (in Table 2), $\mathbb{E}[Z_{(1)}]$ decreases rapidly toward zero, particularly under higher values of $\boldsymbol{\zeta}$. This behavior reflects a strong left-tail concentration and suggests the suitability of the DGM distribution for modeling early failures. Conversely, $\mathbb{E}[Z_{(n)}]$ increases monotonically with n and eventually stabilizes at finite values, revealing the bounded right-tail characteristics of the distribution under specific parameter settings. These trends confirm the flexibility of the DGM model in capturing both early-failure and long-survival phenomena, depending on the configuration of $\boldsymbol{\zeta}$.

4. Likelihood estimation

Assume that just the first m failure times, represented by $z_{1:m} < z_{2:m} < \cdots < z_{m:m}$, are logged when n things go through a life-testing experiment. This set is known as a Type–II censored sample and symbolized by $\mathbf{z} = (z_{1:m}, z_{2:m}, \ldots, z_{m:m})$. The rest of the $n - m$ elements are restricted to only have failure times greater than $z_{m:m}$. In this part, we use the maximum likelihood estimation (MLE) approach to estimate the DGM($\boldsymbol{\zeta}$) model's parameters. Let $\mathbf{z}$ be a Type–II censored sampling from the DGM model. We now define the likelihood function (say, $\mathcal{L}(\cdot)$) of such censored data as follows:

$$\mathcal{L}(\boldsymbol{\zeta}|\mathbf{z}) \propto \prod_{i=1}^{m} P(z_{i:n})[1 - F(z_{m:n}; \boldsymbol{\zeta})]^{n-m}. \tag{4.1}$$

Referring to the PMF and CDF in Eqs (2.3) and (2.4), respectively, the likelihood and the log-likelihood functions are explored as follow:

$$\mathcal{L}(\boldsymbol{\zeta}|\mathbf{z}) \propto \prod_{i=1}^{m} \left[\Delta(z_i; \boldsymbol{\zeta}) - \Delta(z_{i+1}; \boldsymbol{\zeta})\right] e^{(n-m)\left(-\alpha z_m - \frac{\theta}{\mu}(e^{\mu z_m} - 1)\right)}, \tag{4.2}$$

and

$$\log \mathcal{L}(\boldsymbol{\zeta}|\mathbf{z}) \propto \sum_{i=1}^{m} \log\left[\Delta(z_i; \boldsymbol{\zeta}) - \Delta(z_{i+1}; \boldsymbol{\zeta})\right] - (n-m)\left(\alpha z_m + \frac{\theta}{\mu}(e^{\mu z_m} - 1)\right), \tag{4.3}$$

respectively, where z_i is used instead of $z_{i:m}$ for simplicity.

The respective normal equations of α, θ, and μ, such as $\mathcal{L}^{\star}(\cdot) \propto \log \mathcal{L}(\cdot)$, are as follows:

$$\frac{\partial \mathcal{L}^{\star}}{\partial \alpha} = \sum_{i=1}^{m} \left\{ \frac{\Delta(z_{i+1}; \boldsymbol{\zeta}) z_{i+1} - \Delta(z_i; \boldsymbol{\zeta}) z_i}{\Delta(z_i; \boldsymbol{\zeta}) - \Delta(z_{i+1}; \boldsymbol{\zeta})} \right\} - z_m(n-m), \tag{4.4}$$

$$\frac{\partial \mathcal{L}^{\star}}{\partial \theta} = \sum_{i=1}^{m} \left\{ \frac{(\Delta(z_i; \boldsymbol{\zeta}) \nabla^{\circ}(z_i; \mu) - \Delta(z_{i+1}; \boldsymbol{\zeta}) \nabla^{\circ}(z_{i+1}; \mu))}{\Delta(z_i; \boldsymbol{\zeta}) - \Delta(z_{i+1}; \boldsymbol{\zeta})} \right\} + (n-m) \nabla^{\circ}(z_m; \mu), \tag{4.5}$$

and

$$\frac{\partial \mathcal{L}^{\star}}{\partial \mu} = \sum_{i=1}^{m} \left\{ \frac{(\Delta(z_i; \boldsymbol{\zeta}) \nabla^{\bullet}(z_i; \mu) - \Delta(z_{i+1}; \boldsymbol{\zeta}) \nabla^{\bullet}(z_{i+1}; \mu))}{\Delta(z_i; \boldsymbol{\zeta}) - \Delta(z_{i+1}; \boldsymbol{\zeta})} \right\} - (n-m) \nabla^{\bullet}(z_m; \mu), \tag{4.6}$$

respectively, where $\nabla^{\circ}(z_i; \mu) = -\frac{1}{\mu}(e^{\mu z_i} - 1)$ and $\nabla^{\bullet}(z_i; \mu) = -\frac{\theta}{\mu^2}(\mu z_i e^{\mu z_i} + e^{\mu z_i} - 1)$. To ensure the validity of inference for the Type–II censored discrete DGM model, it is necessary to establish that the MLEs $\hat{\boldsymbol{\zeta}}$ exist and are unique. To achieve this, we provide Theorem 3.

Theorem 3. *Let* $\log \mathcal{L}(\boldsymbol{\zeta} \mid \mathbf{z})$*, where* $\mathbf{z}$ *(the vector of the observed ordered failure times) and* $\boldsymbol{\zeta}$ *(the parameter vector) are fixed, be the log-likelihood function of the new DGM distribution under Type–II censoring. Then the MLEs*

$$(\hat{\alpha}, \hat{\theta}, \hat{\mu}) = \arg \max_{(\alpha,\theta,\mu)\in\boldsymbol{\zeta}} \log \mathcal{L}(\boldsymbol{\zeta} \mid \mathbf{z})$$

exist and are unique.

Proof. See Appendix B.

To find the MLE of α, θ, or μ, the offered system of non–linear formulas in (4.4)–(4.6) should be solved numerically. Particularly when working with sums and exponentials, these calculations can be intricate and computationally demanding. For real-world applications, numerical techniques or software programs with symbolic differentiation capabilities could be useful for precisely calculating these derivatives, particularly when maximizing the parameters in real-world situations. Numerous numerical methods have been investigated in the literature; the Newton–Raphson approach of the maxLik package (by Henningsen and Toomet [18]) is used in this investigation. When the initial guess is sufficiently close to the correct solution, the quadratic convergence rate of this method allows for quick refinement of the estimates, which is the main reason it was chosen.

The Fisher information matrix (FIM), which is obtained from the second-order partial derivatives of the log-likelihood function (4.3), is required to generate the matrix of variances and covariances (say, V) of the DGM's model parameters $\boldsymbol{\zeta}$. Each item in the 3×3 symmetric matrix that is the FIM (say, $\mathsf{F}(\cdot)$) represents a second-order partial derivative. The $\mathsf{V}(\cdot)$, represented by $\mathsf{V}(\cdot) \cong \mathsf{F}^{-1}(\cdot)$, is obtained from the inverse of the FIM and used to construct asymptotic confidence intervals (ACIs) for the parameters. The expressions for the $\mathsf{F}(\cdot)$ and $\mathsf{V}(\cdot)$ matrices (at $\boldsymbol{\zeta} = \hat{\boldsymbol{\zeta}}$) are as follows:

$$\widehat{\mathsf{F}}(\hat{\boldsymbol{\zeta}}) = \begin{pmatrix} I_{\alpha\alpha} & I_{\alpha\theta} & I_{\alpha\mu} \\ & I_{\theta\theta} & I_{\theta\mu} \\ & & I_{\mu\mu} \end{pmatrix}_{(\boldsymbol{\zeta}=\hat{\boldsymbol{\zeta}})}, \tag{4.7}$$

and

$$\widehat{\mathsf{V}}(\hat{\boldsymbol{\zeta}}) = \begin{pmatrix} \widehat{\mathrm{var}}(\hat{\alpha}) & \widehat{\mathrm{cov}}(\hat{\alpha},\hat{\theta}) & \widehat{\mathrm{cov}}(\hat{\alpha},\hat{\mu}) \\ & \widehat{\mathrm{var}}(\hat{\theta}) & \widehat{\mathrm{cov}}(\hat{\theta},\hat{\mu}) \\ & & \widehat{\mathrm{var}}(\hat{\mu}) \end{pmatrix}, \tag{4.8}$$

respectively; for brevity, the FIM items associated with $\boldsymbol{\zeta}$ are listed in Appendix C.

Using (4.8), at a preassigned a-th confidence percentage, the two $(1-a)100\%$ ACI bounds of α (as an example) are given by

$$\left(\hat{\alpha} - z_{\frac{a}{2}}\sqrt{\widehat{\mathrm{var}}(\alpha)}, \hat{\alpha} + z_{\frac{a}{2}}\sqrt{\widehat{\mathrm{var}}(\alpha)}\right),$$

where $z_{\frac{a}{2}}$ is the critical value from the standard normal distribution. In a similar fashion, the two $(1-a)100\%$ ACI bounds of θ and μ can be easily derived.

5. Bayes estimation

This section deals with Bayesian estimation, which is applied to estimate the unknown parameters of the DGM model. This method treats the parameters as random variables following a certain model, referred to as the prior distribution. Since prior information is often unavailable, it becomes necessary to choose a suitable prior. A joint conjugate prior distribution is selected for the parameters α, θ, and μ, with each parameter being assumed to follow a gamma distribution. Independent gamma priors are dedicated to updating the DGM's parameters, namely α, θ, and μ, due to their associative properties, which simplifies the subsequent computation and facilitates analysis. The gamma distribution also provides the flexibility to capture a wide range of prior assumptions through its shape and rate parameters; see Pradhan and Kundu [19] and Dey et al. [20].

Thus, suppose $\lambda_i \sim Gamma(a_i, b_i)$, where $a_i > 0$ and $b_i > 0$ (because $i = 1, 2, 3$) are non-negative (known) hyperparameters of the specified DGM parameters $(\lambda_1, \lambda_2, \lambda_3) = (\alpha, \theta, \mu)$. Therefore, the respective prior distributions (symbolized by $\vartheta_i(\cdot),\ i = 1, 2, 3$) for α, θ, and μ are

$$\vartheta_1(\alpha) \propto \alpha^{a_1-1} e^{-b_1\alpha},\ \alpha > 0, \tag{5.1}$$

$$\vartheta_2(\theta) \propto \theta^{a_2-1} e^{-b_2\theta},\ \theta > 0, \tag{5.2}$$

and

$$\vartheta_3(\mu) \propto \mu^{a_3-1} e^{-b_3\mu},\ \mu > 0. \tag{5.3}$$

Therefore, combining Eqs (5.1)–(5.3), the joint prior PDF (say, $\Lambda(\cdot)$) of α, θ, and μ becomes

$$\Lambda(\boldsymbol{\zeta}) \propto \alpha^{a_1-1}\theta^{a_2-1}\mu^{a_3-1} e^{-b_1\alpha-b_2\theta-b_3\mu}. \tag{5.4}$$

With the available data, the joint posterior (say, $\mathcal{P}(\cdot)$) of α, θ, and μ is

$$\mathcal{P}(\boldsymbol{\zeta}|\mathbf{z}) = \xi^{-1}\mathcal{L}(\boldsymbol{\zeta}|\mathbf{z}) \times \Lambda(\boldsymbol{\zeta}), \tag{5.5}$$

where $\xi = \int_\alpha \int_\theta \int_\mu \mathcal{L}(\boldsymbol{\zeta}|\mathbf{z}) \times \Lambda(\boldsymbol{\zeta}) \mathrm{d}\alpha \mathrm{d}\theta \mathrm{d}\mu$ is the normalizing factor.

The squared error (SE) loss function has been used to examine the DGM model's parameter estimates. Afterward, to assess the effectiveness of the estimation approaches and investigate how the parameter values affect them, a simulated analysis is done to evaluate the estimators' effectiveness using several metrics, including coverage probability, mean absolute bias, mean square error, average point estimate, and average interval length. The Bayesian estimate of a parameter ζ (say, $\tilde{\zeta}$ for instance) is defined under the SE loss function as the expected value for the joint posterior distribution as

$$\tilde{\zeta} = \xi^{-1} \int_\alpha \int_\theta \int_\mu \mathcal{L}(\boldsymbol{\zeta}|\mathbf{z}) \times \Lambda(\boldsymbol{\zeta}) \mathrm{d}\alpha \mathrm{d}\theta \mathrm{d}\mu. \tag{5.6}$$

It is necessary to employ numerical approaches for calculating the triple integration mentioned in Eq (5.6). To achieve this, we adopted the Markov chain Monte Carlo (MCMC) approach. A suitable R code via the coda package (by Plummer et al. [21]) was developed to execute this process. Applying the survival discretization method leads to the development of the DGM model, whose PMF is defined in Eq (2.3). The joint posterior density under a Type–II censored sample is expressed as follows:

$$\mathcal{P}(\boldsymbol{\zeta}|\mathbf{z}) \propto \alpha^{a_1-1}\theta^{a_2-1}\mu^{a_3-1} e^{-(b_1\alpha+b_2\theta+b_3\mu)} \prod_{i=1}^{m} \left[\Delta(z_i;\boldsymbol{\zeta}) - \Delta(z_{i+1};\boldsymbol{\zeta})\right] e^{(n-m)\left(-\alpha(z_m)-\frac{\theta}{\mu}(e^{\mu z_m}-1)\right)}. \tag{5.7}$$

For the parameters $\boldsymbol{\zeta}$ under the SE loss function, from (5.5), Bayesian analysis goes beyond creating their corresponding conditional posterior functions, respectively, such as

$$\mathcal{P}_1(\alpha|\theta, \mu, \mathbf{z}) \propto \alpha^{a_1-1} e^{-b_1\alpha}\mathcal{L}(\boldsymbol{\zeta}|\mathbf{z}), \tag{5.8}$$

$$\mathcal{P}_2(\theta|\alpha, \mu, \mathbf{z}) \propto \theta^{a_2-1} e^{-b_2\theta}\mathcal{L}(\boldsymbol{\zeta}|\mathbf{z}), \tag{5.9}$$

and

$$\mathcal{P}_3(\mu|\alpha, \theta, \mathbf{z}) \propto \mu^{a_3-1} e^{-b_3\mu}\mathcal{L}(\boldsymbol{\zeta}|\mathbf{z}). \tag{5.10}$$

From (5.8)–(5.10), the Bayes estimators of α, θ, and μ, respectively, are unable to follow any known statistical distribution. The Metropolis–Hastings (M–H) sampler, the key concept of the MCMC family of Bayesian computation techniques, was developed to address this issue. It is advised to assess the highest posterior density (HPD) intervals of the Bayes point estimates. It is helpful to keep in mind that, depending on the data collected and preconceived notions about the parameters, the HPD depicts a range of values where an unknown parameter is likely to exist with a given probability. Unlike approaches that rely on standard distributions, the M–H algorithm does not require that all conditional distributions to belong to an identifiable family of distributions.

Instead, it creates candidate samples using a proposal distribution, which are then accepted or rejected according to an acceptance probability. This acceptance measure guarantees that the Markov chain will converge to the chosen posterior distribution over time. In this part, we select the normal distribution as a candidate density for all DGM parameters. To implement the MCMC technique using M–H sampling to analyze the DGM parameters, follow the steps described in Algorithm 1.

Algorithm 1 The M–H algorithm for estimating the DGM parameters $\boldsymbol{\zeta}$.

Input: Observed data $\mathbf{z}$
Input: Number of iterations $\mathbb{G}$ and its burn-in $\mathbb{G}^{\bullet}$
Input: Proposal (normal) distribution, say $q(\cdot)$
Initialize: Choose the starting values $\alpha^{(0)}, \theta^{(0)}, \mu^{(0)}$ and set $i = 1$
for $i = 1$ to $\mathbb{G}$ **do**
    Step 1: Propose candidate values
    $\alpha^{\star} \sim q_{\alpha}(\cdot \mid \alpha^{(i-1)})$
    $\theta^{\star} \sim q_{\theta}(\cdot \mid \theta^{(i-1)})$
    $\mu^{\star} \sim q_{\mu}(\cdot \mid \mu^{(i-1)})$
    Step 2: Compute the posterior ratios $Q_{\alpha} = \min\left\{1, \frac{\mathcal{P}_1(\alpha^{\star}|\text{data}) \cdot q_{\alpha}(\alpha^{(i-1)}|\alpha^{*})}{\mathcal{P}_1(\alpha^{(i-1)}|\text{data}) \cdot q_{\alpha}(\alpha^{\star}|\alpha^{(i-1)})}\right\}$
    Accept or reject

$$\alpha^{(i)} = \begin{cases} \alpha^{\star}, & \text{with probability } Q_{\alpha}; \\ \alpha^{(i-1)}, & \text{otherwise} \end{cases}$$

    (Update $\theta^{(i)}$ and $\mu^{(i)}$ similarly)
end for
Output: Posterior MCMC iterations $\left\{(\alpha^{(i)}, \theta^{(i)}, \mu^{(i)})\right\}_{i=1}^{\mathbb{G}}$
Output: The $100(1-a)\%$ HPD interval for α
Sort $\{\alpha^{(\mathbb{G}^{\bullet}+1)}, \ldots, \alpha^{(\mathbb{G})}\}$ as $\alpha^{[\mathbb{G}^{\bullet}+1]} \leq \alpha^{[2]} \leq \cdots \leq \alpha^{[\mathbb{G}]}$
Compute $k = [\alpha(\mathbb{G} - \mathbb{G}^{\bullet})]$
Find $\left\{\alpha^{[i]}, \alpha^{[i+(\mathbb{G}-\mathbb{G}^{\bullet}-k)]}\right\}$
(Update HPD of $\theta^{(i)}$ and $\mu^{(i)}$ similarly)

Bayes' visualization tool is useful for assessing prior impact, validating a model's behavior, and ensuring that Bayesian updating is functioning. For this purpose, by collecting a Type–II censored dataset from DGM(1,1,1) with $(n, m) = (100, 50)$ and $a_i = b_i = 1$ for $i = 1, 2, 3$, the density shapes of the likelihood (light blue), prior (light purple), and posterior (darker purple) distributions of α, θ, and μ are plotted and shown in Figure 2. It reveals that all density shapes of α, θ, or μ dominate slightly due to their narrow peaks, pulling the posterior toward the proposed actual values of all DGM parameters. It also supports our normal density, which is suggested as a proposal for each unknown subject, and indicates that the posterior is sharper than the likelihood but broader than the prior, showing proper Bayesian learning from the data.

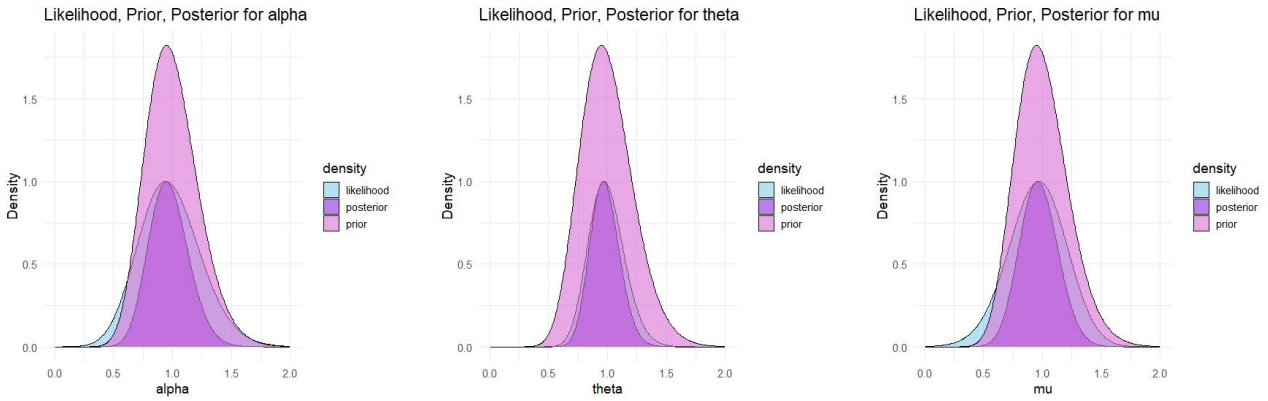

(a) α (b) θ (c) μ

Figure 2. Likelihood, prior, and posterior PDF shapes for the DGM parameters.

6. Simulation comparisons

This section presents a Monte Carlo simulation study designed to assess the performance of the derived estimators of the DGM(ζ) distribution parameters. Following the simulations, we discuss the observed outcomes in detail.

6.1. Simulation design

To generate Type–II censored data from the DGM distribution and to determine the evaluation setup of the proposed estimation methodologies, the simulation proceeds through the steps presented in Algorithm 2. In each iteration of the Monte Carlo simulation, the true parameter values are used as initial guesses to isolate the estimation performance from the initialization effects. This is a common strategy in simulation studies for evaluating the estimator's accuracy. We selected two parameter sets to reflect different distributional behaviors, such as moderate hazard and skewness (in Set–1) and heavier tails and sharper hazard peaks (in Set–2). These choices are based on patterns commonly observed in real reliability and survival data. The sample sizes and censoring levels were designed to mirror practical testing conditions. Without loss of generality, one can easily consider other vectors of the parameter values on the basis of their theoretical domains, as well as other censoring setups in light of their philosophical meaning.

6.2. Simulation results and interpretation

Tables 3–8 report the average point estimate (APE), mean squared error (MSE), mean absolute bias (MAB), average interval length (AIL), and coverage percentage (CP) for each parameter. According to the lowest MSE, MAB, and AIL values and the highest CP values, the following assessments are recorded:

- The estimator's performance improves with increasing n. This indicates the estimator's consistency and robustness. A higher FP% value enhances precision for both point and interval estimations.

- Bayesian estimators outperform their likelihood-based counterparts, confirming their reliability in small samples.
- The HPD interval method outperforms the ACI method due to the additional information gathered by the gamma prior.

Algorithm 2 Monte Carlo simulation algorithm.

Input: True parameter values, DGM($\boldsymbol{\zeta}_0$),
Set–1:DGM(0.1, 0.3, 0.5)
Set–2:DGM(0.5, 1.0, 1.2)
Input: Number of replications $\mathcal{R}$
Input: Sample size $n \in \{30, 60, 100, 150, 200\}$
Input: Failure percentage (FP%) as FP $= \frac{m}{n} \times 100\% \in \{40, 80, 100\%\}$
Input: Prior parameters $(a_i, b_i),\ i = 1, 2, 3,$
For Set–1: $(a_1, a_2, a_3) = (0.5, 1.5, 2.5)$ and $b_i = 5$ for $i = 1, 2, 3$;
For Set–2: $(a_1, a_2, a_3) = (2.5, 5.0, 6.0)$ and $b_i = 5$ for $i = 1, 2, 3$
for each simulation scenario **do**
  for $r = 1$ to $\mathcal{R}$ **do**
    Step 1: Generate n independent uniform variates $u_i \sim U(0, 1)$ for $i = 1, 2, ..., n$
    Step 2: Generate n lifetimes from the DGM($\boldsymbol{\zeta}_0$) distribution, $x_i = F^{-1}(u_i; \boldsymbol{\zeta}_0),\ i = 1, 2, ..., n$
    Step 3: Apply the FP%
    Step 4: Get the point and interval estimations

- MLEs and 95% ACI estimates via maxLik package
- Bayesian and 95% HPD estimates via coda package

    Step 5: Compute

- The APE:

$$\text{APE}(\check{\alpha}) = \mathcal{R}^{-1} \sum_{r=1}^{\mathcal{R}} \check{\alpha}^{(r)}$$

- The MSE:

$$\text{MSE}(\check{\alpha}) = \mathcal{R}^{-1} \sum_{r=1}^{\mathcal{R}} (\check{\alpha}^{(r)} - \alpha)^2$$

- The MAB:

$$\text{MAB}(\check{\alpha}) = \mathcal{R}^{-1} \sum_{r=1}^{\mathcal{R}} |\check{\alpha}^{(r)} - \alpha|$$

- The AIL:

$$\text{AIL}_{95\%}(\alpha) = \mathcal{R}^{-1} \sum_{r=1}^{\mathcal{R}} (\mathcal{U}_{\check{\alpha}^{(r)}} - \mathcal{L}_{\check{\alpha}^{(r)}})$$

- The CP:

$$\text{CP}_{95\%}(\alpha) = \mathcal{R}^{-1} \sum_{r=1}^{\mathcal{R}} \mathbb{I}_{[\mathcal{L}_{\check{\alpha}^{(r)}}, \mathcal{U}_{\check{\alpha}^{(r)}}]}(\alpha),$$

  where $\check{\alpha}^{(r)}$ is the estimate of α at r-th sample.

  end for
end for
Output: Redo Step 5 for β and θ

- Two information priors consistently yield better estimates across parameters due to their lower variances, resulting in more informative posteriors.
- Estimators perform better using Set–1 than with Set–2.
- When $\boldsymbol{\zeta}$ increases, we have the following
  - The MSE, MAB, and AIL values of α, θ, or μ increased;

– All CP values of ζ decreased.

- Under extreme conditions of DGM model parameters, when α, θ, or μ are close to small values, numerical instabilities may appear and lead to increased numerical instability, such as wider confidence intervals and slower convergence.
- Bayes' method and its HPD interval approach are highly effective for parameter inference, offering a reliable evaluation even with censored (incomplete) observations.

Figures 3–5 visually summarize the simulation outcomes, focusing on the MSE and AIL metrics across different parameter configurations. The plots support and validate the trends and conclusions reported in Tables 3–8.

Table 3. Estimation results of α from Set–1.

n	FP%		MLE			Bayes		95% ACI		95% HPD	
30	40%	0.163	0.091	0.258	0.128	0.077	0.196	0.741	0.931	0.313	0.945
	80%	0.145	0.085	0.254	0.192	0.062	0.172	0.669	0.934	0.298	0.946
	100%	0.191	0.080	0.244	0.140	0.056	0.165	0.615	0.936	0.282	0.947
60	40%	0.217	0.078	0.230	0.127	0.050	0.155	0.609	0.935	0.272	0.947
	80%	0.135	0.072	0.220	0.118	0.044	0.145	0.558	0.937	0.258	0.948
	100%	0.144	0.068	0.211	0.135	0.039	0.134	0.514	0.939	0.250	0.948
100	40%	0.167	0.060	0.189	0.133	0.037	0.126	0.443	0.942	0.229	0.950
	80%	0.137	0.059	0.188	0.103	0.028	0.115	0.402	0.943	0.211	0.951
	100%	0.130	0.055	0.187	0.145	0.025	0.103	0.376	0.945	0.203	0.951
150	40%	0.228	0.054	0.185	0.135	0.022	0.093	0.345	0.946	0.192	0.952
	80%	0.140	0.049	0.181	0.120	0.019	0.083	0.313	0.947	0.189	0.952
	100%	0.130	0.039	0.165	0.148	0.016	0.077	0.282	0.949	0.179	0.953
200	40%	0.182	0.036	0.163	0.146	0.013	0.072	0.225	0.952	0.156	0.955
	80%	0.139	0.032	0.154	0.130	0.010	0.068	0.183	0.954	0.141	0.956
	100%	0.172	0.029	0.147	0.128	0.006	0.061	0.132	0.956	0.128	0.958

Table 4. Estimation results of α from Set–2.

n	FP%		MLE			Bayes		95% ACI		95% HPD	
30	40%	0.578	0.748	0.800	0.488	0.140	0.374	0.760	0.929	0.545	0.937
	80%	0.554	0.741	0.780	0.476	0.138	0.357	0.685	0.932	0.527	0.938
	100%	0.481	0.691	0.765	0.487	0.132	0.346	0.632	0.934	0.518	0.938
60	40%	0.560	0.612	0.724	0.556	0.127	0.321	0.626	0.933	0.506	0.939
	80%	0.541	0.598	0.695	0.541	0.121	0.294	0.578	0.935	0.496	0.940
	100%	0.540	0.232	0.397	0.522	0.112	0.279	0.537	0.937	0.468	0.942
100	40%	0.543	0.231	0.395	0.529	0.106	0.253	0.470	0.939	0.444	0.943
	80%	0.519	0.221	0.393	0.519	0.095	0.221	0.435	0.941	0.412	0.945
	100%	0.528	0.220	0.389	0.532	0.089	0.218	0.420	0.943	0.389	0.947
150	40%	0.540	0.220	0.380	0.518	0.084	0.185	0.371	0.944	0.356	0.947
	80%	0.523	0.195	0.352	0.479	0.074	0.184	0.342	0.945	0.328	0.949
	100%	0.533	0.195	0.345	0.488	0.071	0.178	0.330	0.946	0.314	0.949
200	40%	0.537	0.181	0.335	0.518	0.069	0.171	0.294	0.949	0.254	0.952
	80%	0.502	0.179	0.326	0.489	0.065	0.162	0.277	0.951	0.229	0.953
	100%	0.485	0.177	0.322	0.516	0.061	0.158	0.263	0.952	0.202	0.955

Table 5. Estimation results of θ from Set–1.

n	FP%		MLE			Bayes		95% ACI		95% HPD	
30	40%	0.248	0.067	0.272	0.280	0.053	0.246	0.446	0.931	0.305	0.938
	80%	0.262	0.062	0.246	0.239	0.048	0.220	0.389	0.934	0.295	0.939
	100%	0.255	0.058	0.231	0.324	0.043	0.214	0.358	0.936	0.286	0.940
60	40%	0.248	0.054	0.211	0.316	0.038	0.193	0.328	0.937	0.271	0.941
	80%	0.204	0.052	0.202	0.286	0.034	0.184	0.296	0.938	0.262	0.942
	100%	0.264	0.051	0.193	0.386	0.032	0.176	0.265	0.940	0.246	0.943
100	40%	0.223	0.048	0.182	0.346	0.031	0.172	0.243	0.941	0.227	0.944
	80%	0.270	0.047	0.177	0.307	0.024	0.154	0.222	0.942	0.210	0.944
	100%	0.219	0.045	0.173	0.274	0.018	0.132	0.210	0.942	0.181	0.946
150	40%	0.221	0.042	0.169	0.368	0.017	0.125	0.201	0.943	0.135	0.948
	80%	0.289	0.039	0.168	0.324	0.015	0.118	0.192	0.944	0.119	0.950
	100%	0.211	0.035	0.162	0.283	0.008	0.108	0.180	0.944	0.098	0.951
200	40%	0.222	0.033	0.158	0.279	0.006	0.098	0.151	0.946	0.085	0.952
	80%	0.250	0.032	0.156	0.313	0.003	0.088	0.144	0.947	0.074	0.952
	100%	0.200	0.030	0.153	0.285	0.001	0.082	0.128	0.949	0.056	0.953

Table 6. Estimation results of θ from Set–2.

n	FP%		MLE			Bayes		95% ACI		95% HPD	
30	40%	0.890	0.595	0.764	0.936	0.233	0.380	0.736	0.921	0.476	0.932
	80%	0.728	0.518	0.717	0.928	0.198	0.362	0.699	0.924	0.447	0.933
	100%	0.733	0.479	0.687	0.950	0.169	0.345	0.673	0.925	0.413	0.935
60	40%	0.913	0.451	0.668	1.030	0.147	0.335	0.624	0.927	0.384	0.937
	80%	0.704	0.412	0.625	1.012	0.137	0.314	0.584	0.929	0.350	0.938
	100%	0.864	0.347	0.588	1.051	0.112	0.306	0.545	0.931	0.328	0.940
100	40%	0.935	0.313	0.549	1.132	0.103	0.291	0.474	0.933	0.284	0.941
	80%	0.727	0.303	0.525	1.094	0.098	0.288	0.458	0.934	0.278	0.941
	100%	0.622	0.259	0.506	0.904	0.095	0.272	0.423	0.934	0.266	0.942
150	40%	0.939	0.207	0.437	0.951	0.094	0.261	0.378	0.936	0.255	0.943
	80%	0.735	0.184	0.421	0.905	0.091	0.258	0.352	0.936	0.226	0.945
	100%	0.840	0.168	0.395	0.919	0.090	0.253	0.314	0.938	0.216	0.946
200	40%	0.942	0.142	0.329	0.936	0.086	0.251	0.276	0.940	0.198	0.947
	80%	0.743	0.129	0.285	1.071	0.083	0.245	0.233	0.941	0.184	0.949
	100%	0.610	0.115	0.266	1.141	0.079	0.224	0.220	0.942	0.161	0.950

Table 7. Estimation results of μ from Set–1.

n	FP%		MLE			Bayes		95% ACI		95% HPD	
30	40%	0.470	0.589	0.678	0.511	0.293	0.426	0.815	0.925	0.089	0.964
	80%	0.467	0.544	0.655	0.547	0.253	0.401	0.765	0.928	0.082	0.965
	100%	0.468	0.510	0.628	0.525	0.230	0.384	0.739	0.930	0.079	0.965
60	40%	0.508	0.487	0.588	0.537	0.213	0.361	0.697	0.932	0.072	0.966
	80%	0.522	0.459	0.538	0.515	0.184	0.340	0.666	0.935	0.065	0.967
	100%	0.477	0.424	0.519	0.525	0.139	0.308	0.629	0.936	0.062	0.967
100	40%	0.391	0.387	0.483	0.547	0.129	0.298	0.596	0.937	0.060	0.968
	80%	0.421	0.352	0.478	0.527	0.108	0.287	0.562	0.938	0.058	0.968
	100%	0.592	0.325	0.435	0.489	0.099	0.269	0.554	0.939	0.056	0.968
150	40%	0.462	0.287	0.418	0.473	0.088	0.252	0.532	0.940	0.055	0.969
	80%	0.376	0.231	0.375	0.497	0.076	0.238	0.516	0.942	0.053	0.969
	100%	0.563	0.166	0.347	0.503	0.073	0.226	0.468	0.944	0.052	0.969
200	40%	0.441	0.122	0.293	0.467	0.068	0.218	0.396	0.946	0.051	0.970
	80%	0.391	0.110	0.256	0.497	0.061	0.212	0.311	0.949	0.047	0.971
	100%	0.511	0.099	0.244	0.521	0.053	0.201	0.255	0.952	0.043	0.971

Table 8. Estimation results of μ from Set–2.

n	FP%		MLE			Bayes		95% ACI		95% HPD	
30	40%	0.822	0.598	0.696	1.317	0.396	0.581	1.254	0.910	0.149	0.961
	80%	0.848	0.563	0.659	1.377	0.369	0.543	1.195	0.913	0.133	0.962
	100%	1.082	0.524	0.633	1.216	0.345	0.524	0.928	0.915	0.123	0.962
60	40%	0.964	0.496	0.596	1.348	0.328	0.485	0.864	0.918	0.117	0.963
	80%	0.956	0.463	0.564	1.234	0.307	0.456	0.802	0.919	0.106	0.963
	100%	1.192	0.432	0.522	1.217	0.288	0.424	0.768	0.920	0.094	0.964
100	40%	0.961	0.398	0.491	1.144	0.256	0.403	0.716	0.921	0.083	0.965
	80%	0.959	0.364	0.488	1.240	0.236	0.372	0.685	0.922	0.072	0.965
	100%	1.143	0.345	0.464	1.101	0.224	0.342	0.641	0.924	0.067	0.966
150	40%	0.973	0.326	0.444	1.136	0.204	0.313	0.613	0.925	0.062	0.966
	80%	0.966	0.289	0.427	1.215	0.173	0.287	0.574	0.927	0.058	0.966
	100%	1.168	0.278	0.412	1.135	0.148	0.267	0.527	0.928	0.055	0.967
200	40%	0.984	0.263	0.394	1.238	0.128	0.260	0.451	0.930	0.050	0.967
	80%	1.039	0.245	0.389	1.155	0.119	0.247	0.403	0.932	0.047	0.968
	100%	1.270	0.236	0.376	1.197	0.102	0.229	0.350	0.935	0.044	0.968

(a) MSE

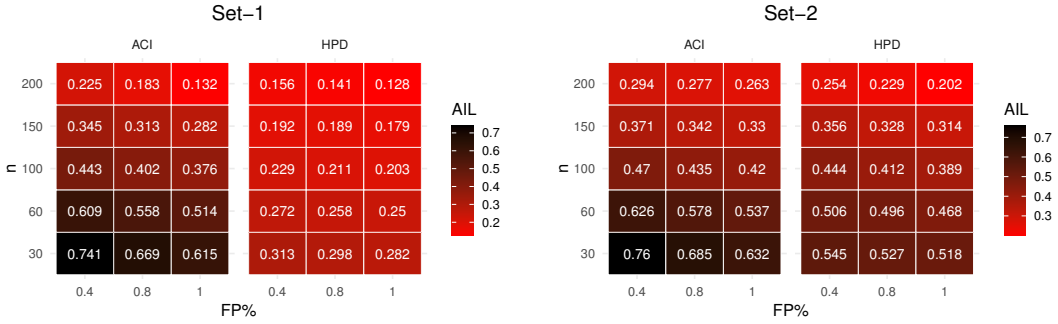

(b) AIL

Figure 3. Plotting the estimation results of α.

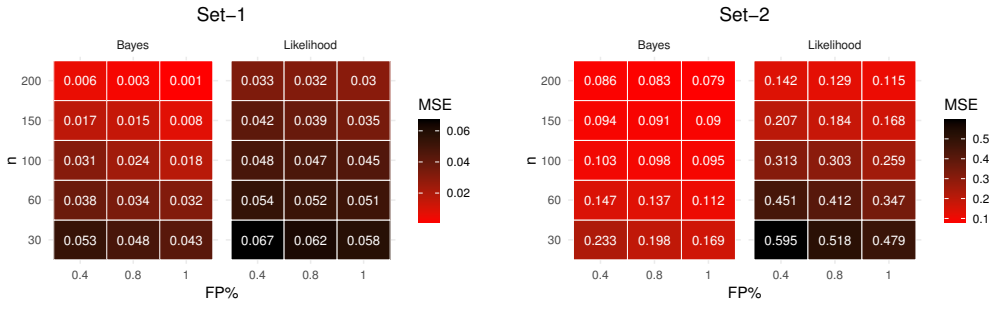

(a) MSE

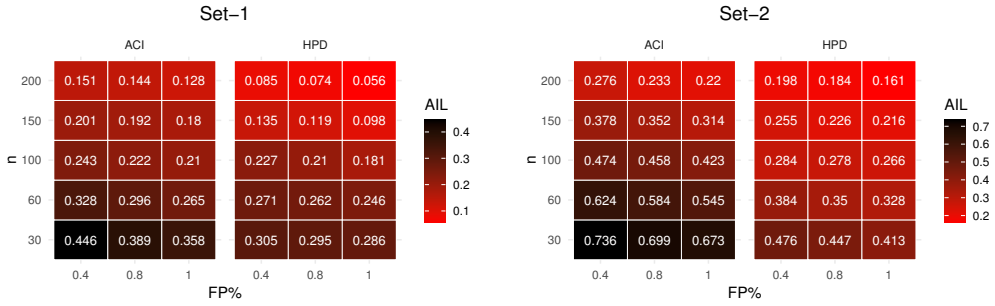

(b) AIL

Figure 4. Plotting the estimation results of θ.

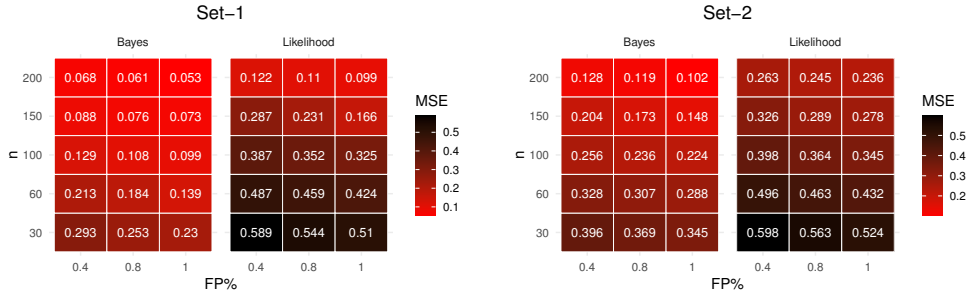

(a) MSE

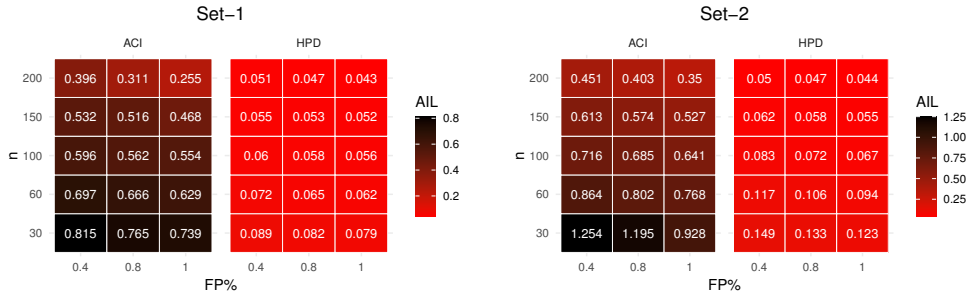

(b) AIL

Figure 5. Plotting the estimation results of μ.

7. Multidisciplinary data analysis

This section analyzes three real-world datasets from distinct domains in turn to (i) assess the proposed model's adaptability and effectiveness in real-world scenarios, (ii) illustrate how its inferential results can be applied to practical contexts, and (iii) evaluate whether it outperforms 10 other existing discrete models from the literature. Table 9 outlines the next datasets as follows:

- Data A: Remission periods (in weeks) for 20 leukemia patients randomly assigned to a specific therapy, originally presented by Bakouch et al. [22].
- Data B: Failure times for 18 electronic devices, first introduced by Wang [23] and later analyzed by Elshahhat and Abu El Azm [24], and Mohammed et al. [25].
- Data C: Total monthly rainfall from January 2000 to February 2007 recorded at Carrol, a rain gauge station in New South Wales, Australia; see Jodra et al. [26] and Alotaibi et al. [27].

Although discrete distributions are ideally applied to datasets with integer-valued support, it is common in the recent statistical literature to use continuous data with small positive values and limited decimal precision (typically one or two decimal places) when fitting newly proposed discrete lifetime models. This is particularly appropriate when the data originate from measurements taken at coarse or discrete time intervals, where the observed values can reasonably approximate countable units. Examples of this approach can be found in studies by Aboraya et al. [28], El-Helbawy et al. [29], and Haj Ahmad and Elshahhat [30], among others. In our case, the datasets labeled A and B comprise low-resolution continuous values, which display clear clustering around integer-like values. This characteristic supports their interpretation as discrete in practice and justifies their use in evaluating the performance of the proposed DGM distribution.

Table 9. Time points in the three data applications.

Data	Time									
A	1	3	3	6	7	7	10	12	14	15
	18	19	22	26	28	29	34	40	48	49
B	5	11	21	31	46	75	98	122	145	165
	196	224	245	293	321	330	350	420		
C	12.0	22.7	75.5	28.6	65.8	39.4	33.1	84.0	41.6	62.3
	52.5	13.9	15.4	31.9	32.5	37.7	9.50	49.9	31.8	32.2
	50.2	55.8	20.4	5.90	10.1	44.5	19.7	6.40	29.2	42.5
	19.4	23.8	55.2	7.70	0.80	6.70	4.08	73.8	5.10	7.60
	25.7	50.7	59.7	57.2	29.7	32.0	24.5	71.6	15.0	17.7
	8.20	23.8	46.3	36.5	55.2	37.2	33.9	53.9	51.6	17.3
	85.7	6.60	4.70	1.80	98.7	62.8	59.0	76.1	67.9	73.7
	27.2	39.5	6.90	14.0	3.00	41.6	49.5	11.2	17.9	12.7
	0.80	21.1	24.5							

The proposed datasets (reported in Table 1) offer a strong variety from medical (Data A), engineering (Data B), and environmental (Data C) fields, demonstrating the model's applicability across domains. Each dataset reflects real-world complexity and includes non-normal, discrete data—ideal for testing the model's flexibility and performance. Their prior use in the literature also allows for fair benchmarking against existing models. Due to the numerical structure of the proposed DGM distribution or its competitors, each model-fitting procedure requires data values that naturally align with its discrete support and parameter space.

However, the original datasets A, B, and C have actual magnitudes that fall outside the effective convergence range for reliable fit calculations. To solve this problem and enable model fit, we applied simple rescaling: The values in Datasets A and C were divided by 10, and the values in Dataset B by 100. This transformation preserves the shape of the data and their relative differences while making them mathematically consistent with the DGM model. All results are interpreted according to the rescaled units.

Table 10 summarizes the key statistics for Datasets A, B, and C, including the minimum, maximum, quartiles (Q_i, $i = 1, 2, 3$), mean, mode, standard deviation (St.D.), skewness, and kurtosis. These results highlight the practical flexibility of the DGM distribution. The consistently positive skewness indicates its suitability for modeling right-skewed data, while the elevated kurtosis reflects the model's capacity to capture heavy tails and pronounced peakedness—characteristics that are particularly relevant in reliability applications.

Moreover, the variance-to-mean ratio demonstrates that the DGM distribution can accommodate both overdispersion and underdispersion, enhancing its adaptability in comparison with classical models such as the Poisson model.

Table 10. Statistics for the three data applications.

Data	Minimum	Maximum	Quartiles			Mode	Mean	St.D.	Skewness	Kurtosis
			Q_1	Q_2	Q_3					
A	0.10	4.90	0.70	1.65	2.83	0.30	1.96	1.47	0.65	2.38
B	0.05	4.20	0.53	1.55	2.81	0.05	1.72	1.32	0.31	1.85
C	0.08	9.87	1.40	3.18	5.12	0.08	3.39	2.37	0.56	2.49

A violin plot combines a boxplot with a density curve to show both the summary statistics and the full distribution shape of the data. So, before seeing the outperformance of the proposed DGM model compared to others, a violin diagram of the three datasets A, B, and C is shown in Figure 6. It indicates that Dataset C has the widest spread and right skew, indicating higher variability and more extreme values compared with the more symmetric and concentrated distributions of Datasets A and B.

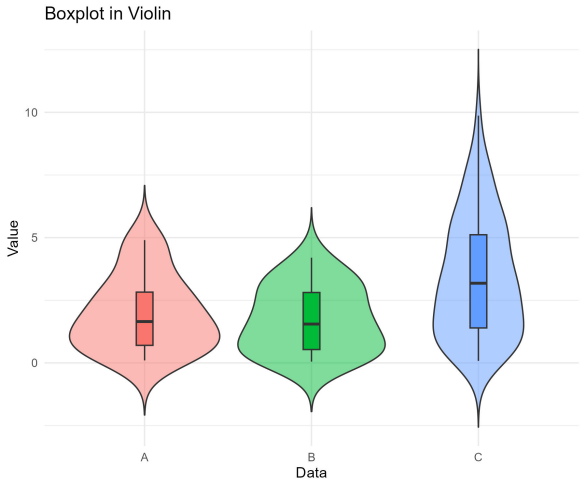

Figure 6. Violin diagram for the three datasets.

To show the utility and flexibility of the newly developed DGM model, for each dataset listed in Table 9, the fitting outcomes of the DGM model are compared with 10 other comparable models from the literature, namely:

- Discrete Hjorth (DH(α, θ, μ)), Haj Ahmad and Elshahhat [30];
- Discrete exponentiated Chen (DEC(α, θ, μ)), Alotaibi et al. [31];
- Exponentiated discrete Weibull (EDW(α, θ, μ)), Nekoukhou and Bidram [32];
- Discrete modified Weibull (DMW(α, θ, μ)), Almalki and Nadarajah [33];
- Discrete Nadarajah-Haghighi (DNH(α, θ, μ)), Shafqat et al. [34];
- Discrete Burr Type XII (DB(θ, μ)), Krishna and Pundir [35];
- Discrete Perks (DP(θ, μ)), Tyagi et al. [36];
- Discrete Weibull (DW(θ, μ)), Nakagawa and Osaki [37];
- Discrete gamma (DG(θ, μ)), Chakraborty and Chakravarty [38];
- Discrete Burr Hatke (DBH(μ)), El-Morshedy et al. [39].

To identify the best-performing model, several evaluation metrics are applied: negative log–likelihood (N–LL), the Akaike information criterion (Ak.), consistent Akaike (CAk.), Bayesian information criterion (BIC), Hannan–Quinn (HQ), and the Kolmogorov–Smirnov (KS) statistic, along with its associated P-value. Table 11 presents the MLE estimates of the parameters α, θ, and μ, including their standard errors (Std.Ers), across all proposed datasets. This table also lists the values of each model evaluation criterion. Across all applications considered, the DGM distribution consistently achieves the lowest scores for every model selection metric—except for the KS statistic, where it records the highest P-value among the competing models. These results indicate that the DGM model provides the best fit and outperforms the other models evaluated.

Table 11. Fitting summary for the DGM and its competitors for the three real applications.

Model	α		θ		μ		N-LL	Ak.	CAk.	B	HQ	KS	
	Est.	Std.Er	Est.	Std.Er	Est.	Std.Er						Distance	P-value
Data A													
DGM	0.419	0.116	0.003	0.004	1.337	0.376	31.592	69.183	70.683	72.171	69.766	0.074	0.999
DH	0.295	0.081	12.68	22.60	0.762	1.551	33.083	72.166	73.666	75.153	72.749	0.164	0.655
DEC	0.786	0.970	0.414	0.241	6.807	13.90	33.651	73.302	74.802	76.290	73.886	0.241	0.195
EDW	0.613	0.755	1.237	1.257	2.138	4.621	33.684	73.368	74.868	76.355	73.951	0.169	0.617
DMW	0.983	0.029	8.326	15.49	1.584	0.189	35.720	77.440	78.940	80.427	78.023	0.218	0.296
DNH	0.000	0.000	19.35	27.20	0.014	0.020	35.067	74.134	74.840	76.126	74.523	0.117	0.949
DB	0.000	0.000	6.959	6.875	0.187	0.186	36.152	76.303	77.009	78.295	76.692	0.285	0.077
DP	0.000	0.000	1.002	0.267	0.131	0.119	34.434	72.868	73.574	74.860	73.257	0.189	0.471
DW	0.000	0.000	1.823	0.341	2.765	0.367	33.762	71.524	72.230	73.515	71.913	0.222	0.280
DG	0.000	0.000	1.189	0.427	2.916	0.988	33.659	71.318	72.024	73.310	71.707	0.241	0.196
DL	0.000	0.000	0.000	0.000	0.219	0.036	32.497	69.993	70.755	72.399	69.988	0.221	0.281
Data B													
DGM	0.433	0.137	0.004	0.006	1.668	0.493	25.375	56.751	58.465	59.422	57.119	0.095	0.991
DH	0.282	0.146	0.082	3.307	0.043	0.163	28.888	63.776	65.490	66.447	64.144	0.188	0.493
DEC	0.246	0.362	0.673	0.296	1.611	1.878	28.752	63.504	65.219	66.176	63.873	0.214	0.332
EDW	0.994	0.012	3.897	1.260	0.331	0.159	28.496	62.991	64.705	65.662	63.359	0.200	0.415
DMW	0.984	0.033	7.682	17.46	1.770	0.288	29.405	64.809	66.524	67.481	65.178	0.208	0.369
DNH	0.000	0.000	20.58	24.54	0.015	0.018	29.584	63.169	63.969	64.950	63.414	0.140	0.826
DB	0.000	0.000	3.961	2.115	0.351	0.192	31.842	67.684	68.484	69.465	67.930	0.262	0.140
DP	0.000	0.000	1.089	0.306	0.131	0.129	29.303	62.606	63.406	64.387	62.852	0.198	0.424
DW	0.000	0.000	1.836	0.387	2.499	0.348	28.842	61.683	62.483	63.464	61.929	0.234	0.237
DG	0.000	0.000	1.226	0.485	2.722	1.021	29.112	62.224	63.024	64.004	62.469	0.245	0.195
DL	0.000	0.000	0.000	0.000	0.246	0.043	27.169	57.337	58.873	59.768	57.460	0.256	0.157
Data C													
DGM	0.149	0.109 0.044	0.071		0.362	0.213	176.55	359.10	359.40	366.35	362.01	0.040	0.999
DH	0.079	0.033	0.000	0.586	0.048	0.039	181.98	369.97	370.27	377.22	372.88	0.115	0.221
DEC	0.323	0.194	0.454	0.085	2.980	1.780	181.48	368.96	369.27	376.22	371.88	0.134	0.102
EDW	0.962	0.068	2.023	0.792	0.761	0.468	181.25	368.50	368.81	375.76	371.42	0.113	0.235
DMW	0.986	0.012	8.388	7.494	1.310	0.045	187.71	381.43	381.73	388.68	384.34	0.139	0.081
DNH	0.000	0.000	21.80	81.69	0.008	0.030	184.57	373.14	373.29	377.98	375.08	0.048	0.992
DB	0.000	0.000	7.116	4.375	0.121	0.075	205.37	414.73	414.88	419.57	416.68	0.155	0.038
DP	0.000	0.000	0.585	0.077	0.163	0.072	183.33	370.67	370.82	375.50	372.61	0.117	0.209
DW	0.000	0.000	1.715	0.155	4.370	0.298	181.33	366.67	366.82	371.50	368.61	0.135	0.096
DG	0.000	0.000	0.628	0.107	2.445	0.381	181.94	367.88	368.03	372.72	369.82	0.138	0.086
DL	0.000	0.000	0.000	0.000	0.137	0.012	196.17	374.33	374.38	376.75	375.31	0.193	0.004

Goodness-of-fit visualization tools help you quickly assess how well a theoretical distribution matches your data by showing the alignment or deviation in shape, spread, and tails. They complement statistical tests and make the model fit easier to interpret, diagnose, and communicate visually. We now highlight the superiority of the DGM model using four fitting visualization tools, namely:

(1) Fitted probability lines;
(2) Fitted reliability lines;
(3) Probability–probability (PP);
(4) Quantile–quantile (QQ).

For a better investigation, in Figure 7, we only compared the new DGM with models with high *P*-values. It reveals that the DGM distribution gives the best fit of all applications regarding the estimated PMF, RF, PP, and QQ curves. This fact comes from the estimated PMF line of the DGM model, which captured more data histograms than others, and the estimated RF, PP, or QQ line of the DGM model is close to its theoretical line statistically compared with the others. Moreover, Figure 7 confirms the numerical results provided in Table 11. The findings in Figure 7 (and Table 11) show that the novel DMG distribution outperforms several existing (traditional or novel) statistical models.

To evaluate the resulting frequentist and Bayes' estimators of α, θ, and μ, three Type–II censored datasets are produced (from Datasets A, B, and C reported in Table 9) by altering various choices of m. Each sample yields MLEs (with 95% ACIs) and Bayes estimations (with 95% HPD intervals). All Bayes assessments are carried out by running the MCMC sampler $\mathbb{G} = 50,000$ times and discarding the first $\mathbb{G}^{\bullet} = 10,000$ iterations as burn-in. Due to a lack of previous information regarding the DGM's parameters, we assign $a_i = b_i = 0.001$ for $i = 1, 2, 3$. Table 12 displays the point estimates (with their Std.Ers), as well as the 95% ACI/HPD limits (with their interval widths (IWs)) of α, θ, and μ. For clarity, the initial values of α, θ, and μ are set using their fitted MLEs obtained via the maxNR() function from the maxLik package to ensure reliable convergence. Table 12 implies that the Bayes approach produced better point and interval estimate results than the likelihood method. When m is raised, all estimates of α, θ, or μ perform well since their Std.Er and IW values drop.

To identify the existence and uniqueness of the fitted estimates of $\hat{\alpha}$, $\hat{\theta}$, and $\hat{\mu}$, and to offer insights into the stability and sensitivity of the model estimates, the contour diagrams (displayed in Figure 8) show how the log-likelihood varies as a function of α, θ, and μ. The subplots in Figure 8 created at (n, m) are taken as (20,10), (18,9), and (83,30) using Datasets A, B, and C, respectively. Figure 8 shows that the fitted values of $\hat{\alpha}$, $\hat{\theta}$, and $\hat{\mu}$ of α, θ, and μ, respectively, exist and are unique. These findings support the accuracy and dependability of the estimated values in Table 12, highlighting the model's validity.

It should be noted here that although Figure 8 may give the visual impression of linearity in certain regions due to axis scaling and three-dimensional projection effects, the underlying log-likelihood surface of the DGM distribution is well-behaved and structurally concave in each parameter. This is supported by the strictly monotonic nature of the likelihood function with respect to α, θ, and μ, which ensures that the likelihood function admits a unique maximum under standard regularity conditions. Numerical optimization routines consistently converged to the same solution across multiple initializations, further affirming the global stability and practical identifiability of the estimators. Hence, the estimators are mathematically identifiable and practically stable.

On the other hand, to assess the potential for convergence of the MCMC sequences for α, θ, and μ, Gaussian kernel density and trace plots for the remaining 40,000 MCMC iterations are created using the same Type–II censored samples used previously in Figure 8; see Figure 9. To clarify, in each subplot in Figure 9, the Bayesian estimated and 95% HPD interval limits are represented by solid and dashed lines, respectively. The subplots in Figure 9 confirm the satisfactory convergence behavior. For all given datasets, the posterior iterations of α (or μ) exhibit near symmetry; in contrast, those of θ display positive skewness, reflecting the varying structural properties of their posterior densities.

Using the key metrics investigated in Table 1, Table 13 summarizes several statistics for α, θ, and μ based on 40,000 MCMC iterations. Table 13 confirms the numerical results provided in Table 12, and the same facts are displayed in Figure 9. Finally, the three real-world applications analyzed demonstrated that the new discrete version of the GM model outperformed other models, providing a flexible and statistically feasible alternative for modeling lifespans, particularly in engineering, biomedical, and actuarial contexts, where discrete event times are prevalent.

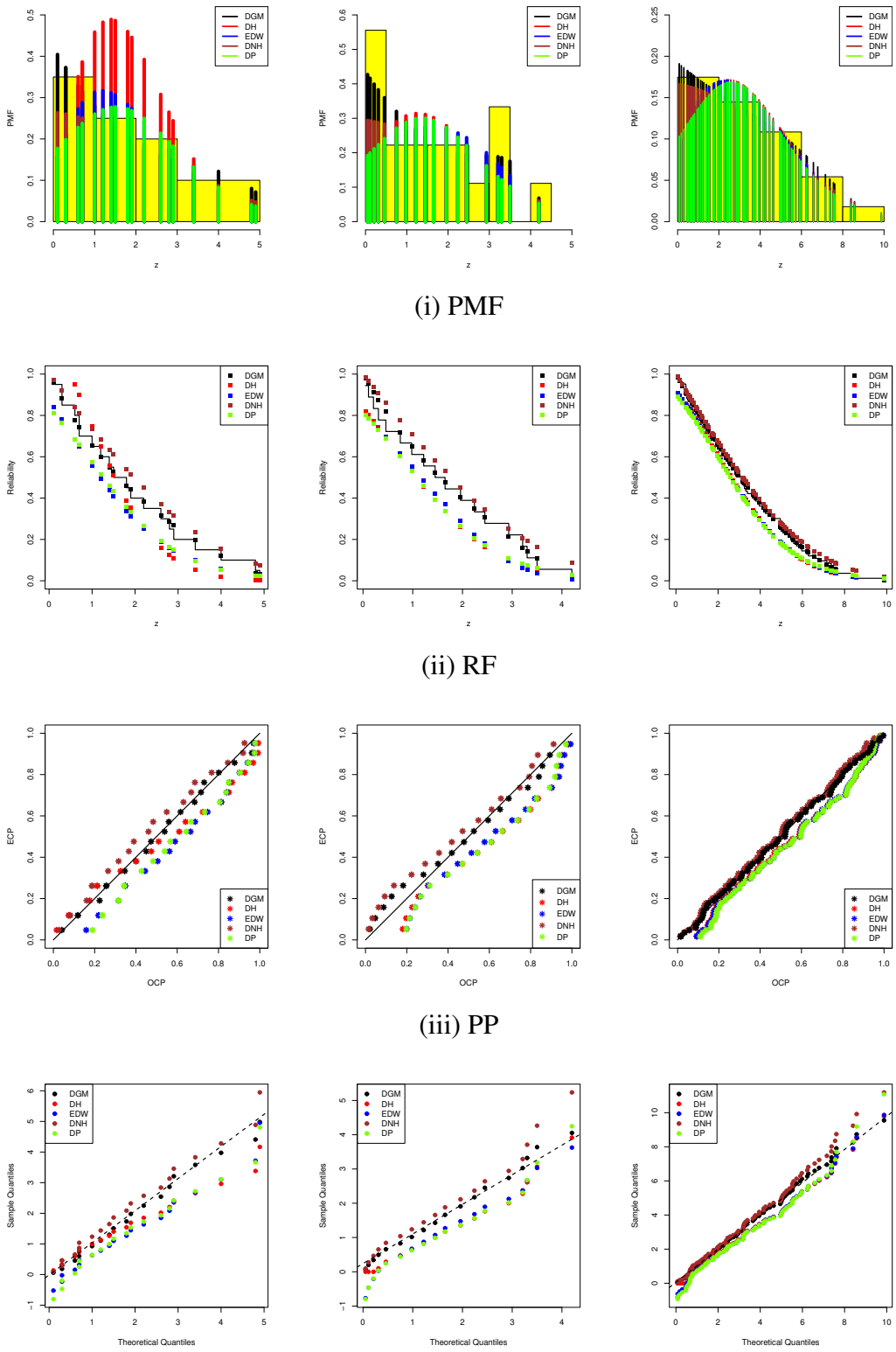

(i) PMF

(ii) RF

(iii) PP

(iv) QQ

(a) Data A (b) Data B (c) Data C

Figure 7. Visualizations of the DGM and its competitors using the three real applications.

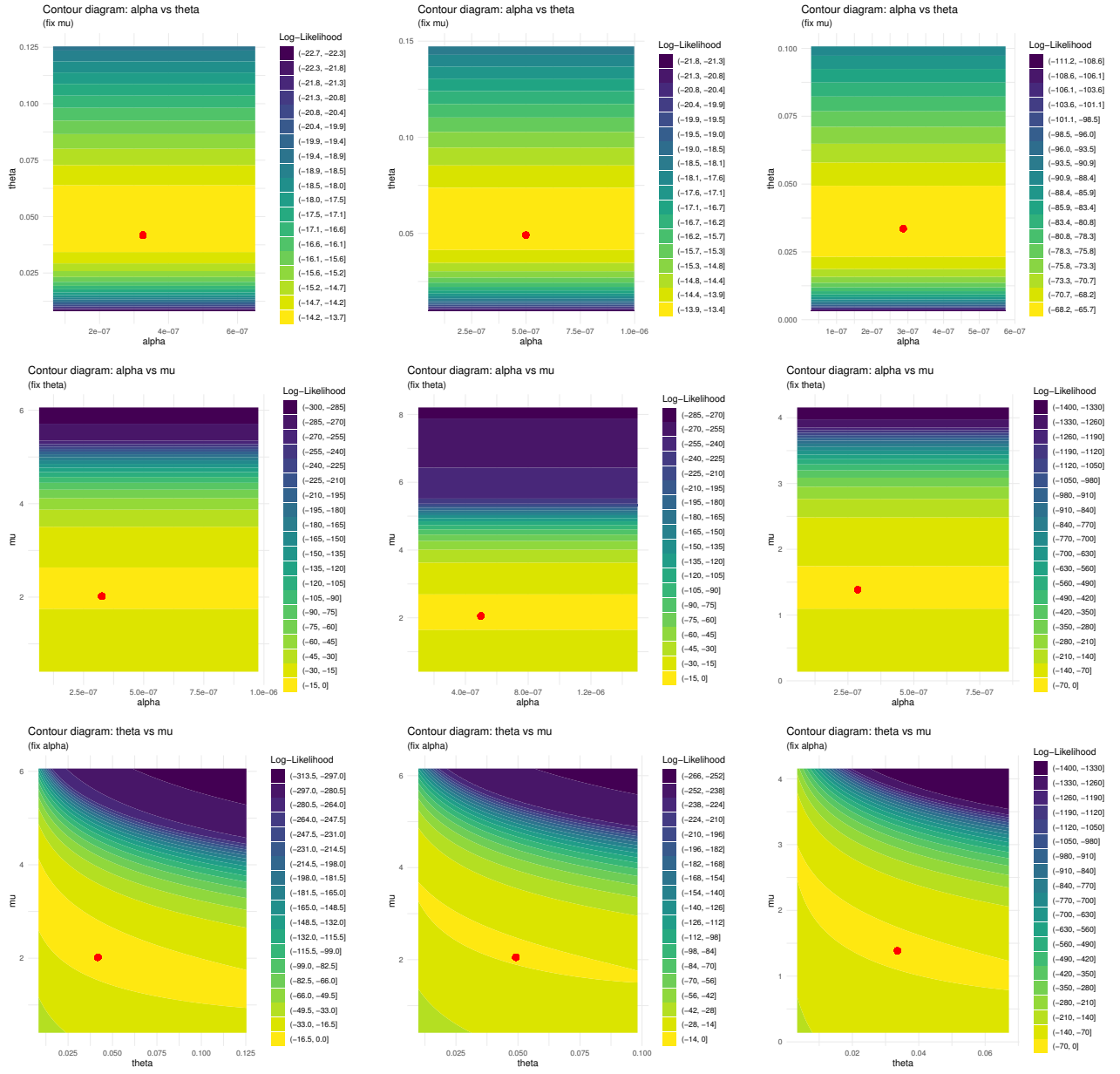

(a) Data A (b) Data B (c) Data C

Figure 8. Contour grids of α (top), θ (center), and μ (bottom) from three genuine datasets.

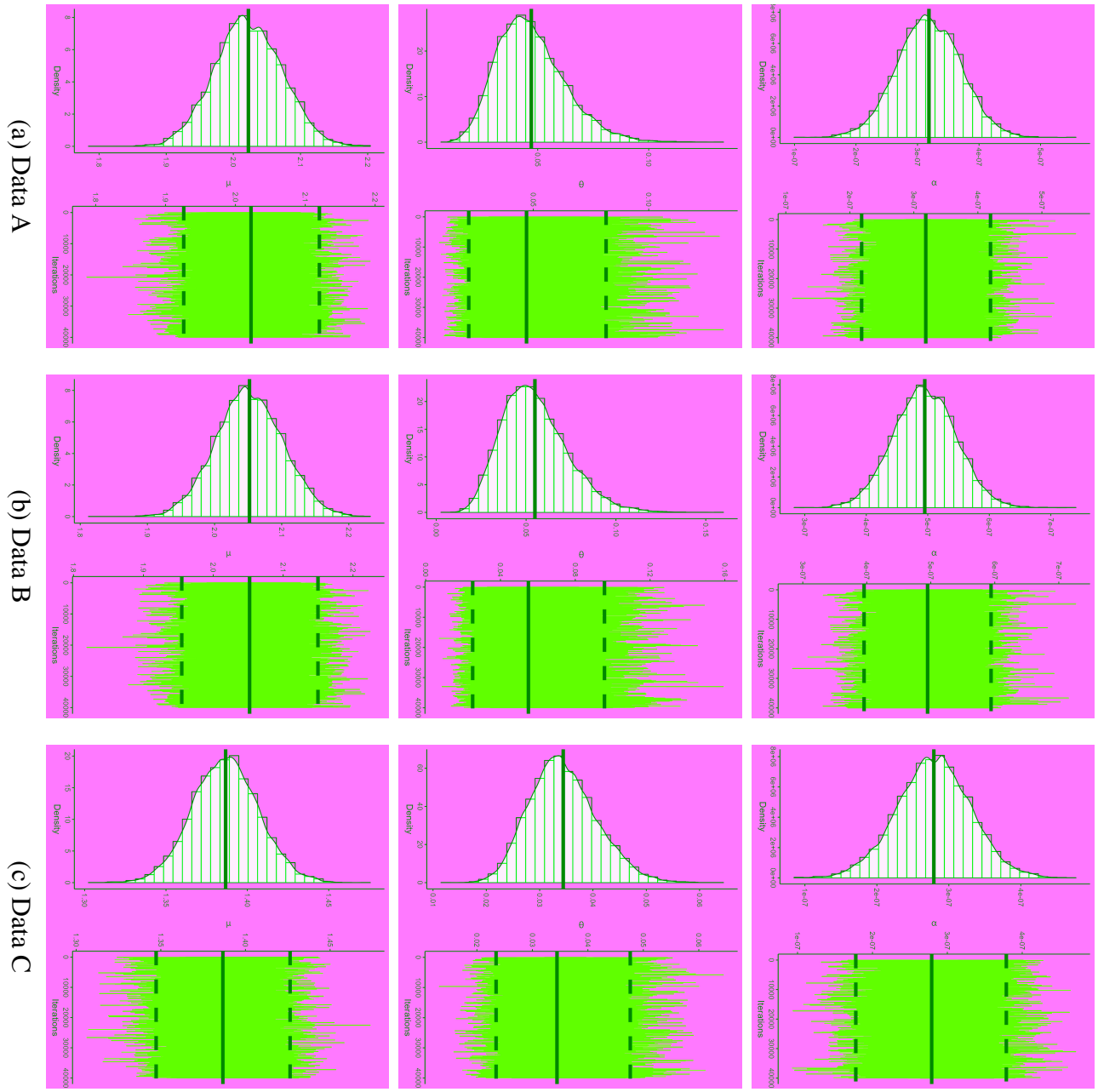

Figure 9. Gaussian kernel with histograms and trace plots of α (right), θ (middle), and μ (left) from three genuine datasets.

Table 12. Estimates of α, θ, and μ from three genuine datasets.

Data	(n,m)	Par.	MLE		Bayes		ACI			HPD		
			Est.	Std.Err	Est.	Std.Err	Low.	Upp.	IL	Low.	Upp.	IL
A	(20,10)	α	3.3E−7	0.1876	3.2E−7	5.2E−8	0.0000	0.3677	0.3677	2.2E−7	4.2E−7	2.0E−7
		θ	0.0418	0.0363	0.0471	0.0162	0.0003	0.1129	0.1126	0.0221	0.0815	0.0595
		μ	2.0199	0.6025	2.0224	0.0499	0.8391	3.2007	2.3617	1.9260	2.1202	0.1942
	(20,15)	α	1.9E−7	0.1730	1.8E−7	5.5E−8	0.0000	0.3392	0.3392	7.1E−8	2.8E−7	2.1E−7
		θ	0.1000	0.0851	0.1084	0.0271	0.0027	0.2668	0.2641	0.0630	0.1626	0.0996
		μ	0.8001	0.3024	0.8015	0.0491	0.2075	1.3928	1.1853	0.7054	0.8986	0.1932
	(20,20)	α	0.4185	0.3401	0.4182	0.0099	0.1918	0.6453	0.4534	0.3989	0.4377	0.0389
		θ	0.0027	0.0645	0.0024	0.0010	0.0002	0.0109	0.0107	0.0004	0.0043	0.0039
		μ	1.3372	0.6136	1.3372	0.0010	0.5994	2.0751	1.4757	1.3352	1.3392	0.0040
B	(18,9)	α	5.0E−7	0.2012	5.0E−7	5.1E−8	0.0000	0.3944	0.3944	4.0E−7	5.9E−7	2.0E−7
		θ	0.0491	0.0522	0.0549	0.0191	0.0053	0.1514	0.1460	0.0251	0.0956	0.0705
		μ	2.0516	0.7011	2.0520	0.0497	0.6776	3.4257	2.7481	1.9550	2.1499	0.1949
	(18,12)	α	2.6E−7	0.2698	2.5E−7	5.2E−8	0.0000	0.5287	0.5287	1.5E−7	3.5E−7	2.0E−7
		θ	0.1327	0.0999	0.1537	0.0397	0.0063	0.3285	0.3222	0.0925	0.2243	0.1317
		μ	0.6548	0.4493	0.6612	0.0498	0.0059	1.5355	1.5296	0.5642	0.7568	0.1926
	(18,18)	α	0.4325	0.3705	0.4323	0.0100	0.1635	0.7015	0.5380	0.4127	0.4518	0.0391
		θ	0.0035	0.0772	0.0033	0.0010	0.0001	0.0152	0.0151	0.0015	0.0051	0.0036
		μ	1.6682	0.7025	1.6682	0.0010	0.7010	2.6354	1.9344	1.6662	1.6702	0.0039
C	(83,30)	α	2.9E−7	0.0681	2.8E−7	5.1E−8	0.0000	0.1334	0.1334	1.8E−7	3.8E−7	2.0E−7
		θ	0.0336	0.0275	0.0344	0.0063	0.0016	0.0874	0.0858	0.0235	0.0476	0.0242
		μ	1.3854	0.3995	1.3867	0.0202	0.6025	2.1684	1.5659	1.3472	1.4264	0.0791
	(83,60)	α	1.7E−7	0.1019	1.6E−7	1.0E−8	0.0000	0.1998	0.1998	1.4E−7	1.8E−7	4.0E−8
		θ	0.0953	0.0770	0.0995	0.0158	0.0026	0.2463	0.2438	0.0720	0.1317	0.0597
		μ	0.3322	0.1392	0.3290	0.0366	0.0594	0.6050	0.5456	0.2582	0.4007	0.1425
	(83,83)	α	0.1489	0.3297	0.1484	0.0095	0.0000	0.3620	0.3620	0.1299	0.1670	0.0371
		θ	0.0435	0.2656	0.0435	0.0010	0.0003	0.1818	0.1815	0.0416	0.0455	0.0039
		μ	0.3619	0.4619	0.3619	0.0010	0.0156	0.7801	0.7645	0.3599	0.3639	0.0039

Table 13. Statistics for α, θ, and μ from three genuine datasets.

Data	(n,m)	Par.	Quartiles			Mode	Mean	St.D.	Skewness
			Q_1	Q_2	Q_3				
A	(20,10)	α	2.84E-7	3.18E-7	3.54E-7	3.19E-7	1.74E-7	5.14E-8	0.01735
		θ	0.03607	0.04539	0.05615	0.04708	0.03267	0.01530	0.66457
		μ	1.98873	2.02087	2.05674	2.02238	2.06454	0.04985	0.04026
	(20,15)	α	1.45E-7	1.80E-7	2.16E-7	1.80E-7	6.70E-9	5.35E-8	-0.07710
		θ	0.09020	0.10679	0.12484	0.10840	0.07137	0.02574	0.37963
		μ	0.76836	0.80064	0.83486	0.80148	0.90005	0.04903	0.00421
	(20,20)	α	0.41153	0.41822	0.42493	0.41822	0.41345	0.00994	0.01564
		θ	0.00180	0.00245	0.00309	0.00244	0.00000	0.00097	-0.04649
		μ	1.33656	1.33725	1.33792	1.33724	1.33464	0.00102	-0.04019
B	(18,9)	α	4.60E-7	4.95E-7	5.29E-7	4.95E-7	5.12E-7	5.07E-8	0.03378
		θ	0.04175	0.05294	0.06602	0.05494	0.04616	0.01820	0.64268
		μ	2.01878	2.05081	2.08548	2.05203	2.05680	0.04966	0.03738
	(18,12)	α	2.20E-7	2.55E-7	2.90E-7	2.55E-7	1.54E-7	5.13E-8	-0.01585
		θ	0.12998	0.15232	0.17572	0.15368	0.13641	0.03372	0.27802
		μ	0.62789	0.66113	0.69517	0.66122	0.69002	0.04939	-0.02159
	(18,18)	α	0.42559	0.43230	0.43906	0.43231	0.44319	0.01000	0.01242
		θ	0.00268	0.00330	0.00393	0.00330	0.00218	0.00092	0.06071
		μ	1.66753	1.66819	1.66888	1.66820	1.66729	0.00100	-0.00315
C	(83,30)	α	2.45E-7	2.79E-7	3.13E-7	2.79E-7	1.94E-7	5.07E-8	-0.02334
		θ	0.03008	0.03397	0.03841	0.03443	0.03388	0.00624	0.37151
		μ	1.37290	1.38658	1.40011	1.38666	1.36567	0.02019	0.04055
	(83,60)	α	1.58E-7	1.65E-7	1.71E-7	1.65E-7	1.58E-7	1.01E-8	-0.00777
		θ	0.08888	0.09864	0.10919	0.09950	0.10735	0.01520	0.32589
		μ	0.30433	0.32919	0.35397	0.32902	0.29384	0.03642	0.02612
	(83,83)	α	0.14196	0.14835	0.15482	0.14839	0.13564	0.00951	0.02243
		θ	0.04282	0.04349	0.04416	0.04350	0.04334	0.00099	0.03055
		μ	0.36121	0.36188	0.36256	0.36188	0.36116	0.00100	-0.00248

8. Conclusions

This paper introduces a novel discrete version of the GM distribution, constructed via survival discretization, and rigorously explores its probabilistic structure, inferential properties, and practical performance across a range of modeling contexts. The new DGM distribution keeps the core properties of the original while making it suitable for data recorded in discrete time. Unlike common discrete models such as the Weibull or gamma models, the DGM can flexibly represent increasing, decreasing, and bathtub-shaped hazard rates, which are often found in survival and reliability data. Both classical maximum likelihood and Bayesian methods are performed to estimate the model's parameters when a dataset with Type–II censoring is available, showing that the model performs well across different sample sizes and data conditions. Simulation studies confirm that Bayesian methods, in particular, provide more reliable estimates when sample sizes are small. Three real-world applications also show that the DGM model fits better than other new discrete versions of common continuous distributions used in practice, namely the modified Weibull, Nadarajah–Haghighi, Burr Type XII, Weibull, and gamma models, and others. Overall, the proposed DGM model is flexible, mathematically simpler, and easy to work with. It improves upon existing discrete lifetime distributions by providing a better fit and more accurate modeling, especially in cases involving censored or incomplete data. Future research could extend this work to more complex settings, such as bivariate or multivariate data. Since L-moments are linear functions of order statistics, they can be derived from the new results and may serve as robust alternatives to conventional moments for summarizing location, scale, and skewness. This direction holds particular promise in applications where classical moments are unstable or sensitive to outliers. Other potential directions include adapting the proposed DGM model to handle more general censoring schemes, like hybrid (or progressive) censoring. Additionally, adding covariates through a regression-based approach would increase the model's usefulness in real-world survival and reliability studies.

Appendix

Appendix A: Log-concavity of the DGM distribution

A discrete distribution with a PMF $P(\cdot)$ is said to be log-concave if it satisfies the following inequality

$$P(z;\boldsymbol{\zeta})^2 \geq P(z-1;\boldsymbol{\zeta}) \cdot P(z+1;\boldsymbol{\zeta}), \quad \text{for all } z \geq 1. \tag{A.1}$$

Equivalently,

$$\Delta(z;\boldsymbol{\zeta})^2 - \Delta(z+1;\boldsymbol{\zeta}) \cdot \Delta(z+1;\boldsymbol{\zeta}) \geq 0. \tag{A.2}$$

It is evident, from (A.2), that the inequality is expressed in a nonlinear form involving the DGM's exponential terms. It is not possible to verify this analytically for all values of z, but we can examine the monotonicity and concavity by analyzing the second-order difference of the natural logarithm of the survival function.

Proof. It is known that if $\Delta(z;\boldsymbol{\zeta})$ is log-convex (i.e., $\log \Delta(z;\boldsymbol{\zeta})$ is convex in z), then the PMF $P(z;\boldsymbol{\zeta})$ is log-concave; see Bagnoli and Bergstrom [40]. To assess the log-concavity of $P(z;\boldsymbol{\zeta})$, from (2.3), we

obtain the second-order difference of $\log \Delta(z;\boldsymbol{\zeta})$ as follows:

$$\log \Delta(z;\boldsymbol{\zeta}) = -\alpha z - \frac{\theta}{\mu}(e^{\mu z} - 1). \tag{A.3}$$

Subsequently,

$$\mathrm{d}^2 \log \Delta(z;\boldsymbol{\zeta}) = \frac{\theta}{\mu} e^{\mu z}(-e^{\mu} + 2 - e^{-\mu}). \tag{A.4}$$

In contrast, the concavity of a function $\Delta(z;\boldsymbol{\zeta})$ is determined using its second-order finite difference, as follows:

$$\mathrm{d}^2 \log \Delta(z;\boldsymbol{\zeta}) := \log \Delta(z+1) - 2\log \Delta(z;\boldsymbol{\zeta}) + \log \Delta(z-1). \tag{A.5}$$

We then get

$$\begin{aligned}
\mathrm{d}^2 \log \Delta(z;\boldsymbol{\zeta}) &= -\alpha(z+1) - \frac{\theta}{\mu}(e^{\mu(z+1)} - 1) - 2\left[-\alpha z - \frac{\theta}{\mu}(e^{\mu z} - 1)\right] + \left[-\alpha(z-1) - \frac{\theta}{\mu}(e^{\mu(z-1)} - 1)\right] \\
&= \frac{\theta}{\mu}\left[-e^{\mu(z+1)} + 2e^{\mu z} - e^{\mu(z-1)}\right], \\
&= \frac{\theta}{\mu}\epsilon(z;\boldsymbol{\zeta}),
\end{aligned}$$

where $\epsilon(z;\boldsymbol{\zeta}) = e^{\mu z}(-e^{\mu} + 2 - e^{-\mu})$.

Note that for all $\mu > 0$, we have $e^{\mu} + e^{-\mu} > 2$, which implies

$$-e^{\mu} + 2 - e^{-\mu} < 0 \quad \Rightarrow \quad \mathrm{d}^2 \log \Delta(z;\boldsymbol{\zeta}) < 0.$$

As a result, $\mathrm{d}^2 \log \Delta(z;\boldsymbol{\zeta}) < 0$, showing that $\log \Delta(z;\boldsymbol{\zeta})$ is concave in z, and hence $\Delta(z;\boldsymbol{\zeta})$ is log-concave. Therefore, the PMF $P(z;\boldsymbol{\zeta})$ in (2.3) is log-concave. □

Appendix B: The existence and uniqueness of the MLEs

Let $(z_1 < z_2 < \cdots < z_m)$ denote the ordered observed failure times under Type–II censoring from the DGM model with the parameters $(\alpha, \theta, \mu) \in (0,\infty)^3$. Then the log-likelihood function

$$\log \mathcal{L}(\boldsymbol{\zeta}|\mathbf{z}) \propto \sum_{i=1}^{m} \log\left[\Delta(z_i;\boldsymbol{\zeta}) - \Delta(z_{i+1};\boldsymbol{\zeta})\right] - (n-m)\left(\alpha z_m + \frac{\theta}{\mu}(e^{\mu z_m} - 1)\right),$$

admits a *unique global maximizer* $(\hat{\alpha}, \hat{\theta}, \hat{\mu}) \in (0,\infty)^3$. Hence, the MLEs $\hat{\boldsymbol{\zeta}} = (\hat{\alpha}, \hat{\theta}, \hat{\mu})^{\top}$ exist and are unique.

Proof. We now establish the existence and uniqueness of the MLEs $\hat{\alpha}, \hat{\theta}, \hat{\mu}$ of the DGM model using Type–II censored data by the following four steps:

- **Step 1. Continuity and differentiability:** The log-likelihood $\log \mathcal{L}(\cdot)$ is composed of finitely many terms of the following form:

$$\log(\psi_i) \equiv \log\left(e^{-A_i(\zeta)} - e^{-A_{i+1}(\zeta)}\right), \quad A_j = \alpha z_j + \frac{\theta}{\mu}(e^{\mu z_j} - 1).$$

  The mapping $\boldsymbol{\zeta} \mapsto A_j$ is C^{∞} smooth (infinitely differentiable) on $(0,\infty)^3$. Since $z_{i+1} > z_i$ implies $A_{i+1} > A_i$, the difference is $e^{-A_i} - e^{-A_{i+1}} > 0$ on $(0,\infty)^3$. Hence, the function $\log \mathcal{L}(\cdot)$ is finite-valued, continuous, and smooth on the open parameter space.

- **Step 2. Boundary behavior:** As $\alpha \to 0^+$ or $\theta \to 0^+$, we have $e^{-\alpha z - \frac{\theta}{\mu}(e^{\mu z}-1)} \approx 1$, so $e^{-A_i} - e^{-A_{i+1}} \approx 0^+$, yielding $\log \psi_i \to -\infty$. Conversely, as any $\boldsymbol{\zeta} \to +\infty$, all terms $e^{-A_j} \to 0$, and again $\psi_i \to 0$ and $\log \psi_i \to -\infty$. Therefore, $\log \mathcal{L}(\cdot) \to -\infty$ on the boundary of $(0,\infty)^3$. Hence any maximizer must lie in the interior.
- **Step 3. Strict concavity:** To prove the uniqueness, we show that $\log \mathcal{L}(\cdot)$ is *strictly concave* in $\boldsymbol{\zeta}$, as follows:
  - The mapping $(A_i, A_{i+1}) \mapsto \log(\psi_i)$ is strictly concave whenever $A_i \neq A_{i+1}$, because it is the logarithm of a positive linear combination of log-convex functions.
  - Each $A_j(\boldsymbol{\zeta})$ is affine in α and convex in (θ, μ) due to the convexity of the exponential map $x \mapsto e^{\mu z_j}$.
  - Composing a strictly concave function with an affine/convex transformation in this manner preserves the strict concavity of $\log(\psi_i)$ in $\boldsymbol{\zeta}$.

  Moreover, the survival term $-(n-m)\Big(\alpha z_m + \frac{\theta}{\mu}(e^{\mu z_m} - 1)\Big)$ is linear in $\boldsymbol{\zeta}$; hence, it does not affect the concavity. Since a finite sum of strictly concave functions is again strictly concave, the full log-likelihood $\log \mathcal{L}(\cdot)$ is strictly concave on the parameter domain $\boldsymbol{\zeta}$.
- **Step 4. Existence and uniqueness.** Combining the existence (ensured by continuity (Step 1) and the boundary divergence (Step 2)) with the uniqueness (ensured by strict concavity (Step 3)), we conclude that:
  - $\log \mathcal{L}(\cdot)$ is continuous on $(0,\infty)^3$ and tends to $-\infty$ at the boundary,
  - $\log \mathcal{L}(\cdot)$ is strictly concave on $(0,\infty)^3$.

Consequently, the log-likelihood function $\log \mathcal{L}(\cdot)$ admits exactly one stationary point $\hat{\boldsymbol{\zeta}}$ in $(0,\infty)^3$, which is necessarily the unique global maximizer and, therefore, the unique maximum likelihood estimator. Hence, the proposed MLEs $\hat{\boldsymbol{\zeta}}$ for the DGM model's parameters $\boldsymbol{\zeta}$ under Type–II censoring both exist and are unique.

Remark: This proof applies to any Type–II censored sample with at least $m \geq 2$ observed failure times, ensuring $A_{i+1} - A_i > 0$. Hence, the uniqueness of the MLE does not depend on the effective sample size m, provided that $m \geq 2$. □

Appendix C: The FIM items

Form (4.3), the FIM elements of α, θ, and μ (provided in (4.7)) are defined as follows:

$$\frac{\partial \mathcal{L}^\star}{\partial \alpha^2} = \sum_{i=1}^{m} \left\{ \frac{\left[z_i^2 \Delta(z_i;\boldsymbol{\zeta}) - z_{i+1}^2 \Delta(z_{i+1};\boldsymbol{\zeta}) \right]}{\left[\Delta(z_i;\boldsymbol{\zeta}) - \Delta(z_{i+1};\boldsymbol{\zeta}) \right]} - \left(\frac{\left[z_i \Delta(z_i;\boldsymbol{\zeta}) - z_{i+1} \Delta(z_{i+1};\boldsymbol{\zeta}) \right]^2}{\left[\Delta(z_i;\boldsymbol{\zeta}) - \Delta(z_{i+1};\boldsymbol{\zeta}) \right]^2} \right) \right\},$$

$$\frac{\partial \mathcal{L}^\star}{\partial \theta^2} = \sum_{i=1}^{m} \left\{ \frac{\left[(\phi(z_i;\mu))^2 \Delta(z_i;\boldsymbol{\zeta}) - (\phi(z_{i+1};\mu))^2 \Delta(z_{i+1};\boldsymbol{\zeta}) \right]}{\left[\Delta(z_i;\boldsymbol{\zeta}) - \Delta(z_{i+1};\boldsymbol{\zeta}) \right]} - \left(\frac{\left[\phi(z_i;\mu)\Delta(z_i;\boldsymbol{\zeta}) - \phi(z_{i+1};\mu)\Delta(z_{i+1};\boldsymbol{\zeta}) \right]^2}{\left[\Delta(z_i;\boldsymbol{\zeta}) - \Delta(z_{i+1};\boldsymbol{\zeta}) \right]^2} \right) \right\}$$
$$- (n-m) \left(\phi(z_m;\mu) \right)^2,$$

$$\frac{\partial \mathcal{L}^\star}{\partial \mu^2} = \sum_{i=1}^{m} \left\{ \left[\Delta(z_i;\boldsymbol{\zeta}) - \Delta(z_{i+1};\boldsymbol{\zeta}) \right]^{-2} \left[\left(\Delta(z_i;\boldsymbol{\zeta}) \left(-\theta \mu^{-2} \left(\mu z_i e^{\mu z_i} + (e^{\mu z_i} - 1) \right) \right) \right) \right. \right.$$

$$
\begin{aligned}
&- \Delta(z_{i+1};\boldsymbol{\zeta})\left(-\theta\mu^{-2}\left(\mu(z_i+1)e^{\mu z_{i+1}}+(e^{\mu z_{i+1}}-1)\right)\right)\Bigg) \\
&- \left[\Delta(z_i;\boldsymbol{\zeta})\theta\mu^{-2}e^{\mu z_i}(1-(z_i)\mu)-\Delta(z_{i+1};\boldsymbol{\zeta})\theta\mu^{-2}e^{\mu z_{i+1}}(1-(z_i+1)\mu)\right]\Bigg]\Bigg\} \\
&+ (n-m)\left[\left(\theta\mu^{-2}(e^{\mu z_m}(\mu z_m-1)+1)\right)^2-\theta\mu^{-4}[\mu^3 z_m^2 e^{\mu z_m}-2\mu\left(\mu z_m e^{\mu z_m}-e^{\mu z_m}+1\right)]\right],
\end{aligned}
$$

$$
\begin{aligned}
\frac{\partial\mathcal{L}^\star}{\partial\alpha\partial\theta} = \sum\nolimits_{i=1}^{m}\Bigg\{&\frac{[z_i\phi(z_i;\mu)\Delta(z_i;\boldsymbol{\zeta})-z_{i+1}\phi(z_{i+1};\mu)\Delta(z_{i+1};\boldsymbol{\zeta})]}{[\Delta(z_i;\boldsymbol{\zeta})-\Delta(z_{i+1};\boldsymbol{\zeta})]}- \\
&\frac{[z_i\Delta(z_i;\boldsymbol{\zeta})-z_{i+1}\Delta(z_{i+1};\boldsymbol{\zeta})]\,[\phi(z_i;\mu)\Delta(z_i;\boldsymbol{\zeta})-\phi(z_{i+1};\mu)\Delta(z_{i+1};\boldsymbol{\zeta})]}{[\Delta(z_i;\boldsymbol{\zeta})-\Delta(z_{i+1};\boldsymbol{\zeta})]^2}\Bigg\} \\
&- z_m\mu^{-1}(e^{\mu z_m}-1),
\end{aligned}
$$

$$
\begin{aligned}
\frac{\partial\mathcal{L}^\star}{\partial\alpha\partial\mu} = \sum\nolimits_{i=1}^{m}\Bigg\{&[\Delta(z_i;\boldsymbol{\zeta})-\Delta(z_{i+1};\boldsymbol{\zeta})]^{-2}\left[(\theta z_i e^{\mu z_i})\,\Delta(z_i;\boldsymbol{\zeta})-\Delta(z_{i+1};\boldsymbol{\zeta})\,(\theta z_i e^{\mu z_{i+1}})\,(z_i+1)\right] \\
&\times[\Delta(z_i;\boldsymbol{\zeta})-\Delta(z_{i+1};\boldsymbol{\zeta})]-[\Delta(z_i;\boldsymbol{\zeta})(\theta e^{\mu z_i})-\Delta(z_{i+1};\boldsymbol{\zeta})(\theta e^{\mu z_{i+1}})(z_i+1)] \\
&\times[\Delta(z_i;\boldsymbol{\zeta})(-z_i)-\Delta(z_{i+1};\boldsymbol{\zeta})(-z_i-1)]\Bigg\},
\end{aligned}
$$

$$
\begin{aligned}
\frac{\partial\mathcal{L}^\star}{\partial\theta\partial\mu} = \sum\nolimits_{i=1}^{m}\Bigg\{&[\Delta(z_i;\boldsymbol{\zeta})-\Delta(z_{i+1};\boldsymbol{\zeta})]^{-2}\Bigg[\Delta(z_i;\boldsymbol{\zeta})\theta\mu^{-2}e^{\mu z_i}\left((z_i-1)\left(\mu^{-1}(e^{\mu z_i}+1)\right)\right) \\
&- \Delta(z_{i+1};\boldsymbol{\zeta})\theta\mu^{-2}z_i e^{\mu z_{i+1}}\left(\mu^{-1}(e^{\mu z_{i+1}}+1)\right)[\Delta(z_i;\boldsymbol{\zeta})-\Delta(z_{i+1};\boldsymbol{\zeta})] \\
&- [\Delta(z_i;\boldsymbol{\zeta})\,(-\phi(z_i;\mu))-\Delta(z_{i+1};\boldsymbol{\zeta})\,(-\phi(z_{i+1};\mu))] \\
&\times\left[\Delta(z_i;\boldsymbol{\zeta})\theta\mu^{-2}e^{\mu z_i}(1-z_i\mu)-\Delta(z_{i+1};\boldsymbol{\zeta})\theta\mu^{-2}e^{\mu z_{i+1}}(1-(z_i+1)\mu)\right]\Bigg]\Bigg\} \\
&+ (n-m)(\mu-1)\mu^{-2}e^{\mu z_m},
\end{aligned}
$$

where $\Delta(z_i;\boldsymbol{\zeta}) = \exp\left(-\alpha(z_i)-\frac{\theta}{\mu}(e^{\mu z_i}-1)\right)$ and $\phi(z_i;\mu) = \mu^{-1}(e^{\mu z_i}-1)$.

Author contributions

Ahmed Elshahhat: Methodology (equal); software (equal); writing–original draft (equal). Hoda Rezk: Methodology (equal); project administration; writing–review and editing (equal). Refah Alotaibi: Funding acquisition (equal); methodology (equal); writing–original draft (equal); writing–review and editing (equal). All authors have read and agreed to the published version of the manuscript.

Use of Generative-AI tools declaration

The authors declare they have not used Artificial Intelligence (AI) tools in the creation of this article.

Funding

This research was funded by the Princess Nourah bint Abdulrahman University Researchers Supporting Project number (PNURSP2025R50), Princess Nourah bint Abdulrahman University, Riyadh, Saudi Arabia.

Acknowledgments

The authors express their gratitude to Princess Nourah bint Abdulrahman University Researchers Supporting Project number (PNURSP2025R50), Princess Nourah bint Abdulrahman University, Riyadh, Saudi Arabia.

Conflict of interest

The authors declare that they have no conflicts of interest.

References

1. B. Gompertz, On the nature of the function expressive of the law of human mortality and on a new mode of determining the value of life contingencies, *Philos. Trans. R. Soc. Lond.*, **115** (1825), 513–585.
2. W. M. Makeham, On the law of mortality and the construction of annuity tables, *Assurance Magazine J. Inst. Actuar.*, **8** (1860), 301–310.
3. A. W. Marshall, I. Olkin, Gompertz and Gompertz–Makeham distributions, In: *Life distributions: structure of nonparametric, semiparametric, and parametric families*, 2007, 363–398. https://doi.org/10.1007/978-0-387-68477-2_10
4. G. A. Shilovsky, Calculating aging: analysis of survival curves in the norm and pathology, fluctuations in mortality dynamics, characteristics of lifespan distribution, and indicators of lifespan variation, *Biochemistry (Moscow)*, **89** (2024), 371–376. https://doi.org/10.1134/S0006297924020159
5. F. Castellares, S. Patrício, A. J. Lemonte, On the Gompertz–Makeham law: a useful mortality model to deal with human mortality, *Braz. J. Probab. Stat.*, **36** (2022), 613–639. https://doi.org/10.1214/22-BJPS545
6. F. C. D. Souza, Closed-form expressions to Gompertz–Makeham life expectancies: a historical note, *Rev. Bras. Estud. Popul.*, **39** (2022), e0220.
7. T. I. Missov, A. Lenart, Gompertz–Makeham life expectancies: expressions and applications, *Theor. Popul. Biol.*, **90** (2013), 29–35. https://doi.org/10.1016/j.tpb.2013.09.013
8. M. Bajjouk, M. E. Rana, C. R. Ramachandiran, S. Chelliah, Software testing for reliability and quality improvement, *J. Appl. Technol. Innovation*, **5** (2021), 40–46.
9. H. Huang, M. A. Milevsky, T. S. Salisbury, Optimal retirement consumption with a stochastic force of mortality, *Insur. Math. Econ.*, **51** (2012), 282–291. https://doi.org/10.1016/j.insmatheco.2012.03.013

10. D. L. Keefer, S. E. Bodily, Three-point approximations for continuous random variables, *Manage. Sci.*, **29** (1983), 595–609. https://doi.org/10.1287/mnsc.29.5.595

11. C. D. Lai, Issues concerning constructions of discrete lifetime models, *Qual. Technol. Quant. Manage.*, **10** (2013), 251–262. https://doi.org/10.1080/16843703.2013.11673320

12. S. Chakraborty, Generating discrete analogues of continuous probability distributions: a survey of methods and constructions, *J. Stat. Distrib. Appl.*, **2** (2015), 6. https://doi.org/10.1186/s40488-015-0028-6

13. R. K. Hammond, J. E. Bickel, Discretization methods for continuous probability distributions, *Wiley Encycl. Oper. Res. Manage. Sci.*, 2011, 1–13. https://doi.org/10.1002/9780470400531.eorms1103

14. D. Roy, The discrete normal distribution, *Commun. Stat. Theory Methods*, **32** (2003), 1871–1883. https://doi.org/10.1081/STA-120023256

15. D. Roy, Discrete Rayleigh distribution, *IEEE Trans. Reliab.*, **53** (2004), 255–260. https://doi.org/10.1109/TR.2004.829161

16. M. Bebbington, C. D. Lai, M. Wellington, R. Zitikis, The discrete additive Weibull distribution: a bathtub-shaped hazard for discontinuous failure data, *Reliab. Eng. Syst. Safe.*, **106** (2012), 37–44. https://doi.org/10.1016/j.ress.2012.06.009

17. J. E. Cohen, C. Bohk-Ewald, R. Rau, Gompertz, Makeham, and Siler models explain Taylor's law in human mortality data, *Demogr. Res.*, **38** (2018), 773–842. https://doi.org/10.4054/DemRes.2018.38.29

18. A. Henningsen, O. Toomet, maxLik: a package for maximum likelihood estimation in R, *Comput. Stat.*, **26** (2011), 443–458. https://doi.org/10.1007/s00180-010-0217-1

19. B. Pradhan, D. Kundu, Bayes estimation and prediction of the two-parameter gamma distribution, *J. Stat. Comput. Simul.*, **81** (2011), 1187–1198. https://doi.org/10.1080/00949651003796335

20. S. Dey, A. Elshahhat, M. Nassar, Analysis of progressive Type-II censored gamma distribution, *Comput. Stat.*, **38** (2023), 481–508. https://doi.org/10.1007/s00180-022-01239-y

21. M. Plummer, N. Best, K. Cowles, K. Vines, CODA: convergence diagnosis and output analysis for MCMC, *R News*, **6** (2006), 7–11.

22. H. S. Bakouch, M. A. Jazi, S. Nadarajah, A new discrete distribution, *Statistics*, **48** (2014), 200–240. https://doi.org/10.1080/02331888.2012.716677

23. F. K. Wang, A new model with bathtub-shaped failure rate using an additive Burr XII distribution, *Reliab. Eng. Syst. Safe.*, **70** (2000), 305–312. https://doi.org/10.1016/S0951-8320(00)00066-1

24. A. Elshahhat, W. S. Abu El Azm, Statistical reliability analysis of electronic devices using generalized progressively hybrid censoring plan, *Qual. Reliab. Eng. Int.*, **38** (2022), 1112–1130. https://doi.org/10.1002/qre.3058

25. H. S. Mohammed, M. Nassar, A. Elshahhat, A new Xgamma–Weibull model using type-II adaptive progressive hybrid censoring and its applications in engineering and medicine, *Symmetry*, **15** (2023), 1428. https://doi.org/10.3390/sym15071428

26. P. Jodra, M. D. Jimenez-Gamero, M. V. Alba-Fernandez, On the Muth distribution, *Math. Model. Anal.*, **20** (2015), 291–310. https://doi.org/10.3846/13926292.2015.1048540

27. R. Alotaibi, M. Nassar, A. Elshahhat, Rainfall data modeling using improved adaptive Type-II progressively censored Weibull-exponential samples, *Sci. Rep.*, **14** (2024), 1–30. https://doi.org/10.1038/s41598-024-80529-5

28. M. Aboraya, H. M. Yousof, G. G. Hamedani, M. Ibrahim, A new family of discrete distributions with mathematical properties, characterizations, Bayesian and non-Bayesian estimation methods, *Mathematics*, **8** (2020), 1648. https://doi.org/10.3390/math8101648

29. A. A. El-Helbawy, M. A. Hegazy, G. R. Al-Dayian, R. E. Abd EL-Kader, A discrete analog of the inverted Kumaraswamy distribution: properties and estimation with application to COVID-19 data, *Pak. J. Stat. Oper. Res.*, **18** (2022), 297–328.

30. H. Haj Ahmad, A. Elshahhat, A new Hjorth distribution in its discrete version, *Mathematics*, **13** (2025), 875. https://doi.org/10.3390/math13050875

31. R. Alotaibi, H. Rezk, C. Park, A. Elshahhat, The discrete exponentiated-Chen model and its applications, *Symmetry*, **15** (2023), 1278. https://doi.org/10.3390/sym15061278

32. H. Bidram, V. Nekoukhou, The exponentiated discrete Weibull distribution, *Stats. Oper. Res. Trans.*, 2015, 1696–2281.

33. S. J. Almalki, S. Nadarajah, A new discrete modified Weibull distribution, *IEEE Trans. Reliab.*, **63** (2014), 68–80. https://doi.org/10.1109/TR.2014.2299691

34. M. Shafqat, S. Ali, I. Shah, S. Dey, Univariate discrete Nadarajah and Haghighi distribution: properties and different methods of estimation, *Statistica*, **80** (2020), 301–330. https://doi.org/10.6092/issn.1973-2201/9532

35. H. Krishna, P. S. Pundir, Discrete Burr and discrete Pareto distributions, *Stat. Methodol.*, **6** (2009), 177–188. https://doi.org/10.1016/j.stamet.2008.07.001

36. A. Tyagi, N. Choudhary, B. Singh, A new discrete distribution: theory and applications to discrete failure lifetime and count data, *J. Appl. Probab. Statist.*, **15** (2020), 117–143.

37. T. Nakagawa, S. Osaki, The discrete Weibull distribution, *IEEE Trans. Reliab.*, **R-24** (1975), 300–301. https://doi.org/10.1109/TR.1975.5214915

38. S. Chakraborty, D. Chakravarty, Discrete gamma distributions: properties and parameter estimations, *Commun. Stat. Theory Methods*, **41** (2012), 3301–3324. https://doi.org/10.1080/03610926.2011.563014

39. M. El-Morshedy, M. S. Eliwa, E. Altun, Discrete Burr-Hatke distribution with properties, estimation methods and regression model, *IEEE Access*, **8** (2020), 74359–74370. https://doi.org/10.1109/ACCESS.2020.2988431

40. M. Bagnoli, T. Bergstrom, Log-concave probability and its applications, *Econ. Theory*, **26** (2005), 445–469. https://doi.org/10.1007/s00199-004-0514-4

AIMS Press